DOE/MC/30357 -- 5706
(M97005427)

Three-Dimensional Subsurface Imaging Synthetic Aperture Radar (3D SISAR)

Final Report
September 22, 1993 - September 22, 1996

Work Performed Under Contract No.: DE-AC21-93MC30357

For

U.S. Department of Energy
Office of Environmental Management
Office of Technology Development
1000 Independence Avenue
Washington, DC 20585

U.S. Department of Energy
Office of Fossil Energy
Federal Energy Technology Center
Morgantown Site
P.O. Box 880
Morgantown, West Virginia 26507-0880

DISTRIBUTION OF THIS DOCUMENT IS UNLIMITED

By
Mirage Systems
575 Maude Court
Sunnyvale, California 94086-2803

Disclaimer

Abstract

The concept developed under this applied research and development contract is a novel Ground Penetrating Radar system capable of remotely detecting, analyzing, and mapping buried waste containers from a mobile platform. From the testing and analysis performed to date, the 3-D SISAR has achieved the detection, accurate location, and three-dimensional imaging of buried test objects from a stand-off geometry. Tests have demonstrated that underground objects have been located to within 0.1 meter of their actual position.

This work validates that the key elements of the approach are performing as anticipated. The stand-off synthetic aperture radar (SAR) methodology has been demonstrated to be a feasible approach as a remote sensing technique. The radar sensor constructed under this project is providing adequate quality data for imaging, and the matched filters have been demonstrated to provide enhanced target detection. Additional work is on-going in the area of underground propagation and scattering phenomena to provide enhanced depth performance, as the current imaging results have been limited to a few feet of depth underground.

Acknowledgment

Support for this contract has been provided through Messrs. C. Eddie Christy of METC Morgantown and J. Keith Westhusing of the METC Laramie Project Office, the project CORs. The period of performance was 9/93 through 12/95, and the EM focus areas are Contaminant Plume Containment, Remediation, and Land Stabilization.

Table of Contents

Table of Contents, cont'd

Tables

Figures

1.0 Executive Summary

This applied research and development project addressed the development of a novel Ultra Wide Bandwidth (UWB) Ground Penetrating Radar (GPR) sensor system which operates at significant distances from the ground surface to produce three-dimensional (3-D) images of buried objects. A major goal of the project was to advance the state of the art of non-invasive sensor technologies applicable to DOE waste site characterization. The GPR sensor operates from a mobile platform as a spotlight-mode synthetic aperture radar (SAR). Although the project utilized a ground-based platform for the sensor, the system is compact and adaptable to airborne platforms as well.

The use of a stand-off sensor (versus a surface-mounted GPR) allows for more efficient data collection over moderate to large sized regions and eases operation over irregular terrain. In addition, remote stand-off operation is of benefit in certain applications where safety concerns make ground contact operation undesirable, as in the detection and characterization of buried radioactive waste, unexploded ordnance, or mines.

The system operates as a spotlight mode SAR in which the radar sensor continuously illuminates or "stares" at the region to be characterized as the platform motion forms the synthetic aperture. During data collection, the radar traces out a near-circular path around the survey area forming a relatively large 2-D spatial aperture. The UWB radar signal waveform adds the needed space-time diversity in the data to produce high resolution 3-D images of the underground environment. Some other unique features of this system include:

- The radar employs an interrupted, swept-frequency modulation technique that improves the sensitivity of the radar over commonly available conventional impulse GPR's, and improves the immunity to other signals that share the same frequency spectrum.

- A set of three radar signal repeaters were developed to permit measurement of the position of the radar sensor within a few centimeters each time the radar performs a frequency sweep. The position of the repeaters also establishes a reference coordinate system for the objects detected in the underground imaged volume, which enables accurate position estimates to be made for the located objects.

- A modern, easy to use graphical user interface was designed for control of the radar that displays the data for performance monitoring during data collection activities.

The scope of the project work included systems engineering tasks to establish DOE requirements, analyze requirements, develop a GPR specification, and define the test and demonstration activities. A new radar system was specifically designed for GPR operation and installed in the Mirage Test Vehicle (MTV) to provide a demonstration testbed. Signal and image processing software was developed to provide the three-dimensional imaging capability. A purchased

display and visualization program, AVS 5, from Advanced Visual Systems was used for the presentation of the displayed images on a Silicon Graphics workstation. Several means for processing the sensor data were investigated. These included an inverse imaging technique, a method based on tomographic reconstruction, and a specialized matched filter technique. The 3-D imaging to date has been achieved using the matched filter technique. Work on the other processing methods has not yet proceeded far enough to yield images.

The major achievement of this project was demonstrating detection, accurate location, and 3-D imaging of buried objects with a sensor operating at significant standoff ranges from the ground surface. This demonstration has established the basic feasibility of the standoff SAR approach to 3-D characterization of the underground environment.

Although the effort under this contract has been completed, development work is continuing at Mirage to improve the performance of the imaging algorithms at greater depths than demonstrated thus far. The suggested tasks for future work outlined in Para 5.0 should also provide enhanced depth performance. The future work includes additional performance testing at a calibrated DOE site such as Rabbit Valley, Colorado for benchmarking purposes, antenna system modifications, speeding up the image processing through algorithm changes, a faster CPU, or parallel processing methods, and completing the work started at SRI International and the University of Kansas for adapting existing 3-D imaging approaches to the unique data collection geometry of the 3-D SISAR.

2.0 Methodology

2.1 Introduction

This document summarizes the technical investigations performed under this contract. This volume contains the project overview with a summary of the work performed and the conclusions that may be drawn from it. Appendices III through V present the technical approach in substantial detail for those readers wishing to pursue the underground imaging algorithmic concepts and simulation methods at greater technical depth. Listings of all the source code developed under this project are included, along with an 8mm magnetic tape of the software programs.

2.2 Program Overview and Objectives

The purpose of this contract was to develop and demonstrate the feasibility for using advanced ground penetrating radar technology to characterize the subsurface environments at DOE storage sites. The technology developed provides three-dimensional images useful for mapping the location of buried objects and waste materials during pre-remediation characterization and post-remediation monitoring of storage sites.

The scope of this work included systems engineering tasks to establish DOE requirements, perform requirements analyses, develop a GPR specification, and define the test and demonstration activities. An existing instrumentation radar system, suitably modified for GPR operation, was originally proposed as a means to support the demonstration of the GPR techniques being developed. Serious deficiencies with the instrumentation radar led to the development of a new radar system specifically designed for GPR operation, which was installed in the Mirage MTV to provide a demonstration testbed. Signal and image processing software was developed to provide the three-dimensional mapping capability. A purchased display and visualization program, AVS 5, from Advanced Visual Systems was used for the presentation of the displayed images on a Silicon Graphics workstation.

Development and demonstration of this capability required a series of tests to be performed to evaluate the system capabilities. The results of the testing have been used to characterize the system, refine the design, and to develop a plan for additional testing at a DOE site.

2.3 System Level Requirements

An early task in the development of the 3-D SISAR was the definition of the system performance requirements. These were categorized in the following manner, from which elements of the design were derived.

a. Sensor performance requirements. The radar must provide high quality radar data for clear images. At the system level, this requirement translates to

- High system sensitivity in order to capture weak signals from deeply buried objects in lossy soils. High sensitivity is obtained through the use of a low noise receiver and a moderately high system output of 5 Watts effective radiated power (ERP). The relatively high duty cycle of the gated FMCW waveform allows a high average power output.

- High dynamic range in order to see weak signals in presence of strong reflections from clutter. Clutter is defined as any mechanism producing reflections that compete with the desired reflections from the buried objects within the underground region of interest. The system has an exceptionally high instantaneous dynamic range of nearly 90 dB to maximize subclutter visibility.

- A spatially directive antenna radiation pattern for reducing the amplitude of the reflections from surface clutter and below-ground clutter. An antenna pattern of 60° X 60° beamwidth has been tailored to optimally illuminate the imaged region.

- High parameter measurement stability. A coherent detection process provides the stability required for the synthetic aperture integration process and the precision ranging method.

- High immunity to other signals present in the environment. the gated FMCW waveform provides interference rejection.

b. The data collection geometry must be optimized for 3-D imaging with multi-perspective viewing provided by the circular spotlight mode.

- Spatial diversity in collected data is essential to forming a 3-D image. This requirement is satisfied by the circular spotlight mode of operation, which provides up to 30 dB improvement in object detectability through integration of buried objects while suppressing clutter reflections.

- A means of measuring the antenna position in three dimensions to an uncertainty of a few centimeters is needed for SAR operation. This is provided by a set of three reference repeaters placed within the imaged area.

c. The imaging algorithms must account for the unique effects of underground signal propagation.

- Distortions are caused by non-linearity inherent in underground propagation and refraction through the interface at the surface and at interfaces between ground layers. Corrections must be factored into the imaging algorithms for these phenomena.

- Matching the scattering characteristics of buried objects with known response enhances detection and identification. This technique is known as matched filtering.

- Computational efficiency is important due to the large quantity of volume elements (voxels) within the imaged area.

2.3.1 Optimization of System Characteristics for GPR Operation

Through careful design, the 3-D SISAR performance has been optimized for GPR operation. The following discussion outlines the influence of key system performance parameters that have a direct influence on the performance of the 3-D SISAR. In general, the 3-D SISAR performance will be largely governed by the radar sensitivity, radar dynamic range, object scattering characteristics, and the site factors, such as local soil conditions, data collection geometry, clutter environment, and the presence of interference sources.

Sensitivity and SNR. The radar sensitivity determines the maximum amount of loss that can be tolerated from all mechanisms along the radar signal transmission path for a given image quality. For everything else being equal, greater sensitivity translates to greater depth at which objects can be detected and clearly imaged. System sensitivity is a function of receiver noise figure, transmitted power, antenna gain, and stand-off range.

Another parameter is the ratio of the level of the signal that is received by the radar from the scattering object to the sum of all the noise sources as seen by the radar. This ratio is call SNR, or signal-to-noise ratio, and relates a number of operational parameters. There are several sources of noise that will be seen by the radar receiver. First, there is the internal thermal noise generated by the receiver itself. This noise is the sum of the internal losses between the radar antenna and the first gain stage of the radar receiver plus the noise contributed by the receiver amplifiers and mixers. Second, there are noise signals that are collected by the antenna. Atmospheric noise and galactic noise may become significant contributors within the low frequency region of the tuning range of the radar. There are also man-made sources of noise that will be intercepted in urban areas as well as ignition noise from automobiles, etc. Interference can appear as a noise source, and is further described below. There are other sources of noise within the 3-D SISAR system, such as the switching transients generated by the transmit-receive gating function, which add to the receiver

thermal noise and can become the dominate contributors to the receiver noise output unless carefully controlled through design.

Dynamic Range. The stand-off approach has the benefit of not placing the antenna into intimate contact with the ground being imaged, but the elevated radar antenna will be subjected to all of the signals in the environment and additional sources of noise. The directive pattern of the antenna has been tailored to illuminate the area on the ground that is being imaged, and will attenuate signals emanating from other directions to minimize this effect. The antenna design chosen attenuates signals arriving from the sides and the back by about 15 dB on average. These unwanted signals can be either reflections from nearby above-ground objects (clutter), or signals emanating from communications services and TV/FM broadcasting stations. These two sources will produce the strongest environmental signals seen by the radar receiver in an urban environment. Features were incorporated in the radar to enable operation in areas where strong environmental signals may be present. These consist of a capability to blanking of portions of the frequency range where strong interfering signals may exist, and a filter to reduce FM broadcast signal strength.

The imaging performance of the radar depends upon having a sufficiently high dynamic range so that the signals received from the underground objects are not suppressed by the undesired effects of noise, interference, and high-amplitude above-ground reflections from surface clutter. The radar performance parameter that describes the ability of the radar to operate in the presence of these undesired signals is called subclutter visibility, and is directly related to the linear operating range of the receiver. In the 3-D SISAR receiver, great attention was given to achieving the highest possible value of linearity. The term most often used to describe the linear operating range of the radar receiver is called instantaneous dynamic range, or simply dynamic range. It is calculated as the difference between the receiver internal noise level and the strongest signal that the radar can process without internally generating spurious signals.

Integration gain and surface clutter rejection. Integration gain from spotlight mode SAR is between 20 and 30 dB. This gain is due to the coherent integration of the signal energy from all positions along the circular antenna path. The energy from undesired signals does not correlate, and hence an improvement in the signal-to-noise ratio results.

Surface clutter rejection also arises from a process inherent within the FMCW radar technique. In an FMCW radar, the received signal is heterodyned with a sample of the transmitted waveform, producing a beat frequency proportional to range of the detected object. As the distance to a reflecting object grows, the FMCW radar produces a higher and higher difference signal. The bandwidth of the post detection filter is set to pass frequencies only up to the limit corresponding to the radar's designed maximum range, and removes signal echoes from objects that lie beyond. The frequency of signals produced by

objects beyond the desired range, such as surface clutter, are highly attenuated.

Effects of gating the FMCW waveform. The 3-D SISAR employs an on-off gated signal to permit monostatic (single antenna) operation. The transmitted radar waveform consists of a CW signal which sweeps from 20 MHz to 1 GHz. This signal is gated at a very fast rate, governed by the propagation time to the maximum range of the imaged volume containing the buried the objects of interest. For the test and evaluation geometry, the duration of the transmit signal is about 400 nanoseconds. After the signal is transmitted, the radar receives the reflected energy for a corresponding period of time less the time it takes for the antenna and radar hardware to change state, about 100 nanoseconds.

The gating of the FMCW waveform gives rise to two major effects on the radar performance. First, the radar signal modulation spreads the transmitted signal energy over a wide bandwidth, several MHz. The potential for the radar to interfere with other broadcast and communications services is greatly reduced since the signal itself will appear noiselike and only a small portion of this energy will be seen by other receivers. Conversely, any environmental signal received by the radar is modulated by the same process, and its energy is spread over the same bandwidth, thereby reducing the interference to the radar. Much of this modulated received signal energy is rejected by the narrowband post detection filtering (40 kHz wide) within the radar receiver, so that the radar suppresses of interfering signals by about 16 dB.

With the gated radar waveform, the duty cycle (ratio of on to off time) is high, providing more energy that can be used for target detection. The ability of a radar to detect objects is directly proportional to the amount of energy that is available to illuminate the underground region of interest.

The second major effect of the gating of the transmitted signal is that the radar sensitivity is more uniform over the imaged volume, and rapidly drops to zero outside of the desired range extent. The gated signal duration is set so that there is the least amount of loss for the detection of objects at the farthest range extent. Objects at closer ranges will encounter a processing loss proportional to the amount of energy that is not seen by the radar receiver. The amount of energy admitted by the receiver for objects at ranges less than the maximum decreases as R^2 due to this gating loss. This partially compensates for the $1/R^4$ propagation spreading loss through the air as the radar signal travels back and forth to the object or region being imaged. The net system sensitivity as a function of range is therefore proportional to $1/R^2$, rather than $1/R^4$, which enhances the detection of deeper objects.

2.3.2 System Performance Parameters

The generalized requirements were translated to specific system performance parameters. Tradeoffs were performed among interacting parameters to optimize the overall system performance. The resulting system design achieves the performance required to produce high quality radar data for clear images.

Table 2.3.2-1. System Performance Parameters

Parameter	Value
Effective Transmit RF Bandwidth	20-1,000 MHz
Radiated Power	0.5 Watt @ 100 MHz, increasing linearly to 5 Watts @ 350 MHZ and above
System Noise Figure	12 dB
Effective Noise Bandwidth	40 kHz baseband video bandwidth
Directive Antenna Gain	-5 dBi @ 20 MHz, increasing to 6 to 8 dBi above 50 MHz
Dynamic Range	88 dB instantaneous, with 0-24 dB of adjustable RF attenuation
A/D Quantization Level	16 bits
Waveform Flexibility	
Frequency Step Size	Up to 65,536 steps per chirp
Sweep Rate	20 kHz to 10 MHz stepping rate
Sweep duration	Up to 100 milliseconds
Blanking	Programmable over 12 independent frequency ranges
Data Acquisition System Parameters	
Rate	≤160,000 samples/second
Number of Channels	One, with a single I-Q pair of outputs

Appendix II contains additional detail regarding the system performance parameters and the unit level requirements.

2.4 System Architecture

The major hardware components of the 3-D SISAR are the radar unit, antenna and mast, Data Acquisition Subsystem, calibration and support equipment, position reference repeaters, and the Silicon Graphics workstation. Operationally, the system collects data using the arrangement of Figure 2.4-1. The platform carrying the radar sensor and data collection equipment traverses a circular path around the underground area to be imaged. Data is simultaneously collected for the underground imaging algorithms and to determine the position of the radar for each data set. With one traversal of the circle, sufficient data is collected to develop an underground image.

Figure 2.4-2 shows the radar and the antenna attached to the Mirage Test Vehicle. This configuration was used for the field experiments and demonstrations. The antenna and radar subassembly is located at the top of a 45 foot pneumatic mast, a height suitable for standoff operation. The radar signal data is sent down the mast via a high speed digital link to a controller and a data collection subsystem located in the trailer. Figure 2.4-3 is the functional block diagram of the final system configuration. There are several other important new features of this design, such as provisions for adequate performance monitoring and fault isolation, and ruggedness of design to withstand the rigors of field use.

2.4.1 Radar System Development

2.4.1.1 Development Approach

The radar configuration has evolved over the course of the design phase of this project. In an attempt to save development costs and time, the 3-D SISAR radar was originally configured for demonstration purposes from a modified instrumentation radar consisting of several rack-mounted chassis and several pieces of test equipment. As the design phase progressed, it was concluded that, even with the planned enhancements, the radar performance required to support the imaging algorithms would be insufficient to produce clear images for this application. The chief culprit was the long RF transmission lines between the rack-mounted radar equipment and the antenna on top of the mast. These long transmission lines give rise to ringing in the radar signals from slight mismatches in the impedances between the equipment connected at each end of the cable. The ringing can obscure details in the images and leave artifacts that appear as false images, much like "ghosts" in TV reception.

It was determined that the optimum approach to eliminate the cabling delay problems was to locate the RF portion of the radar atop the mast near the antenna, keeping the RF cable lengths very short. This necessitated an all-new design of the radar hardware, since it is impossible to repackage the existing equipment into a compact, lightweight form. Figure 2.4.1-1 shows the mast-mounted radar enclosure, showing the major components arranged in a compact, easy to assemble and repair layout. In function, this unit is the

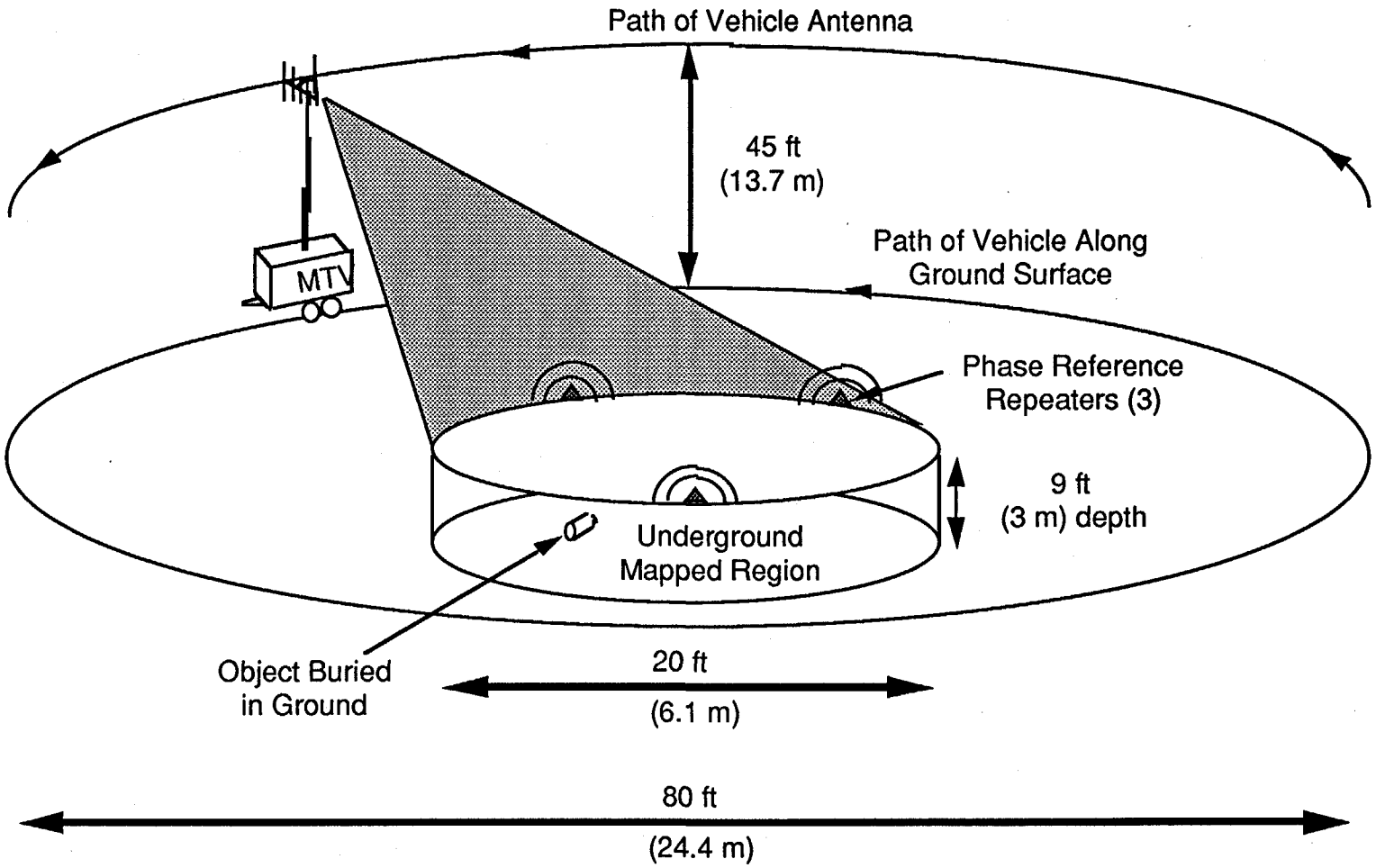

Figure 2.4-1. System data collection geometry.

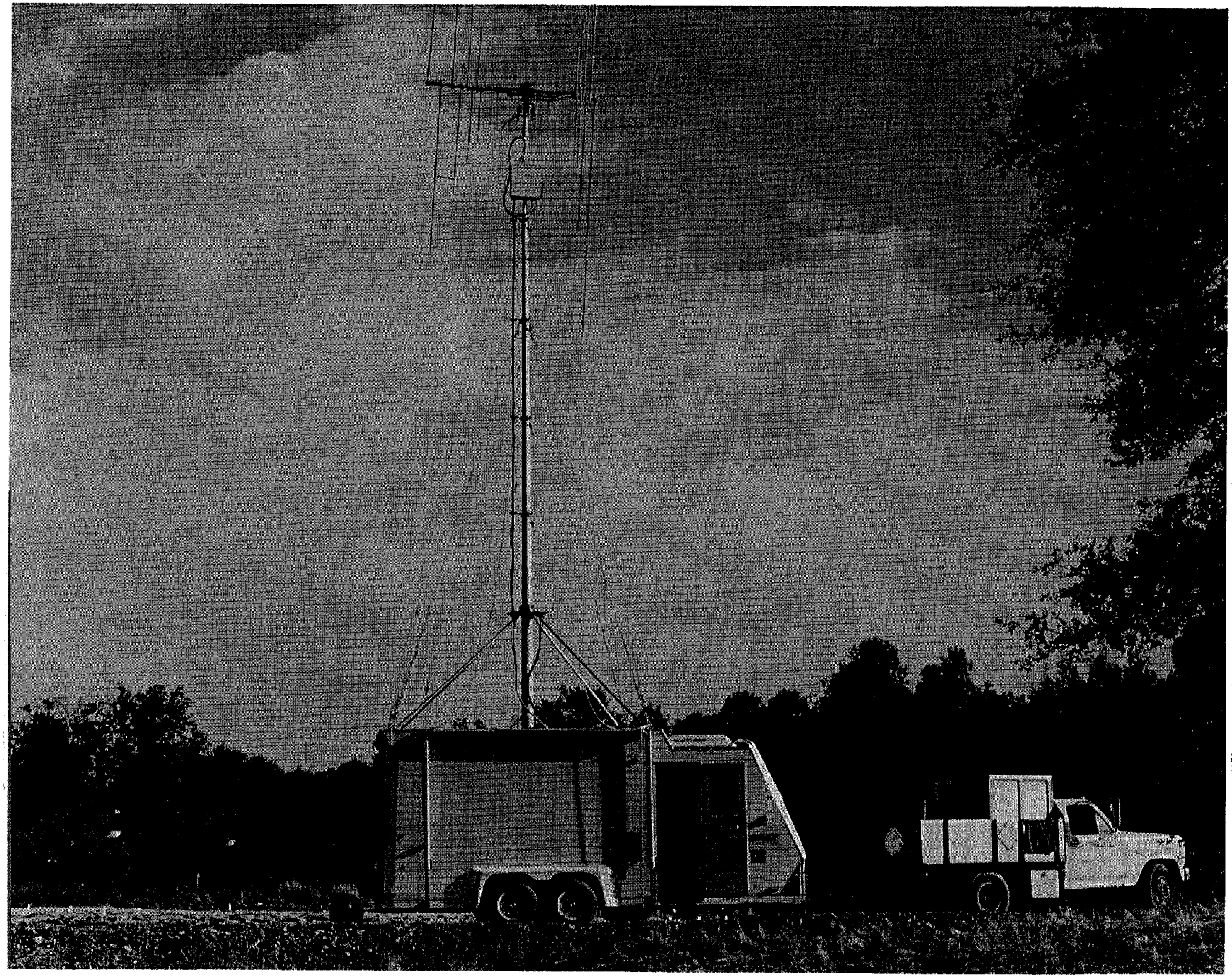

Figure 2.4-2. Mirage Test Vehicle with mast, radar unit, and antenna attached.

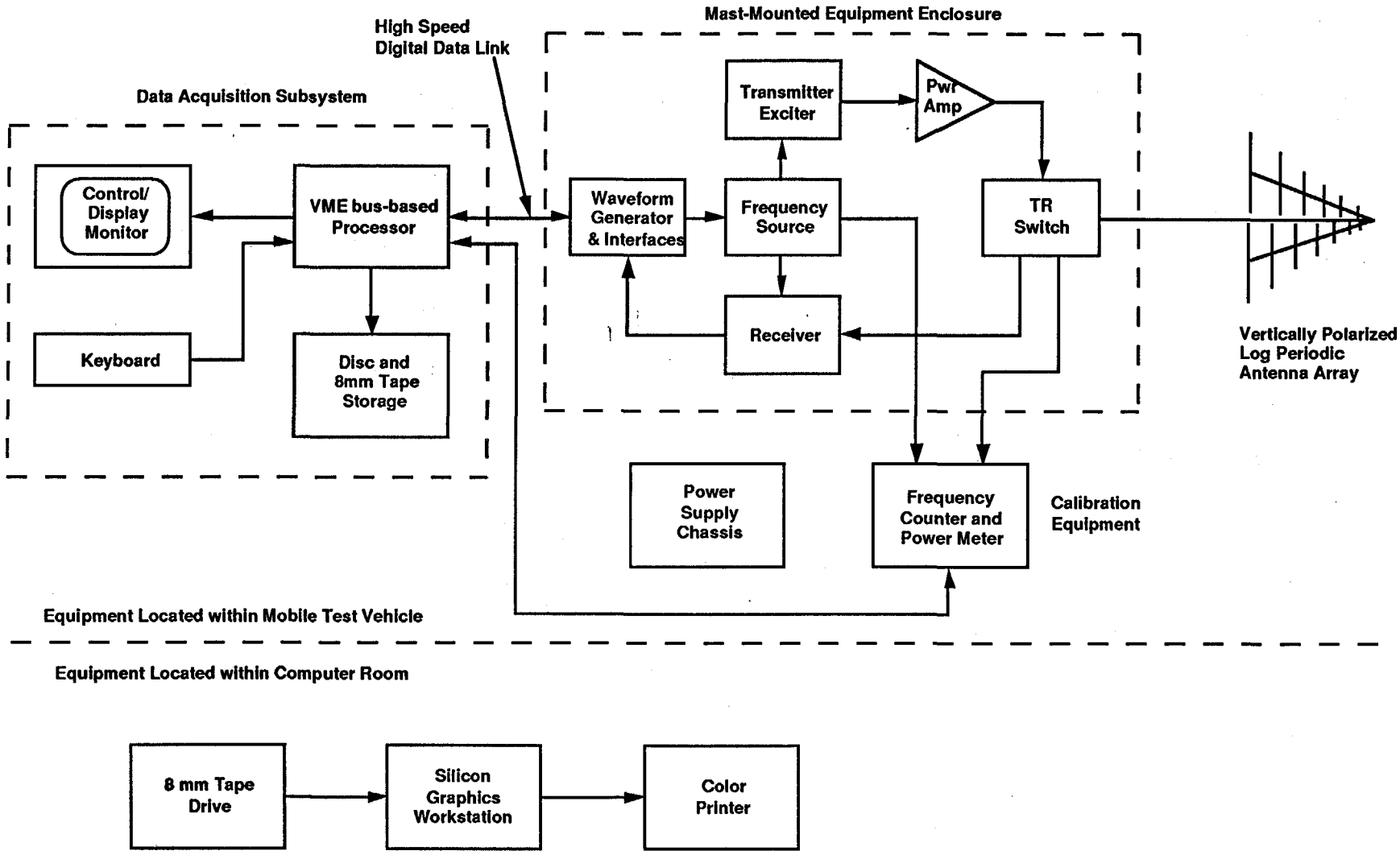

Figure 2.4-3. Functional block diagram of the 3--D SISAR equipment.

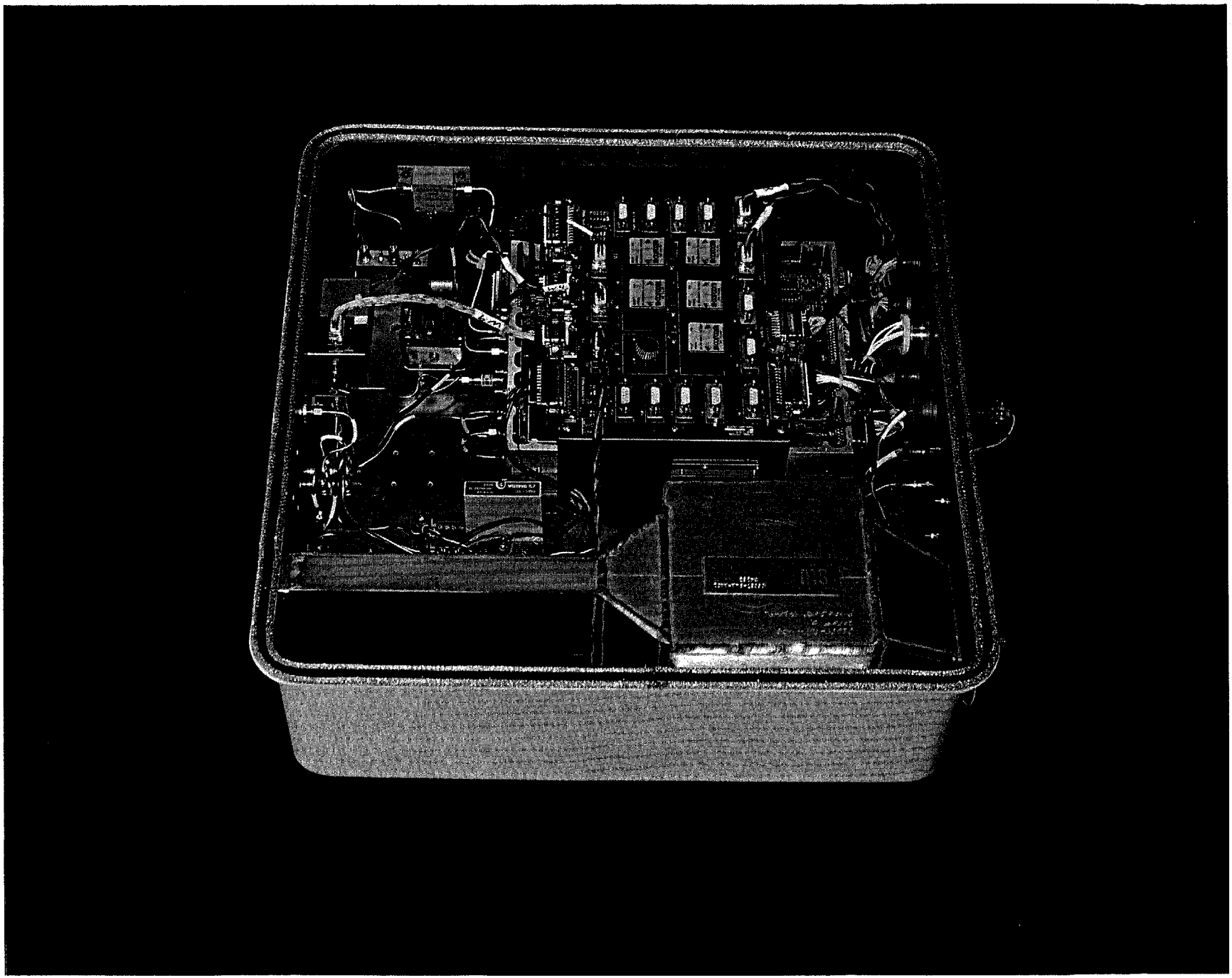

Figure 2.4.1-1. Mast-mounted radar unit.

equivalent of nearly a full rack of equipment, mostly contained in three major subassemblies. The unit is sealed from the environment, and uses an air-to-air heat exchanger so that dirt and moisture do not enter the electronics portion of the unit.

2.4.1.2 Radar Operation

Figure 2.4.1.2-1 shows a simplified block diagram of the radar equipment. The radar uses a frequency modulated, continuous wave (FMCW) waveform in a monostatic (single antenna) mode of operation. The transmitter and receiver are alternately connected to the antenna through a transmit/ receive switch for short periods of time, generally hundreds of nanoseconds to hundreds of microseconds. The waveform generator provides the exciter signal for the transmitter and a replica of that signal to the receiver for use as a reference during signal demodulation. The receiver output is digitized and provides two output paths. The first path consists of real-time processing based on the Fast Fourier Transform (FFT) algorithm. The displayed FFT data allows the operator to monitor the data gathering process. The second path consists of a recording capability for the digitized receiver in-phase and quadrature phase (I and Q) outputs for subsequent computer based 3-D image processing. The signals from the phase reference repeater are embedded within the radar data, and no special hardware is needed to process them.

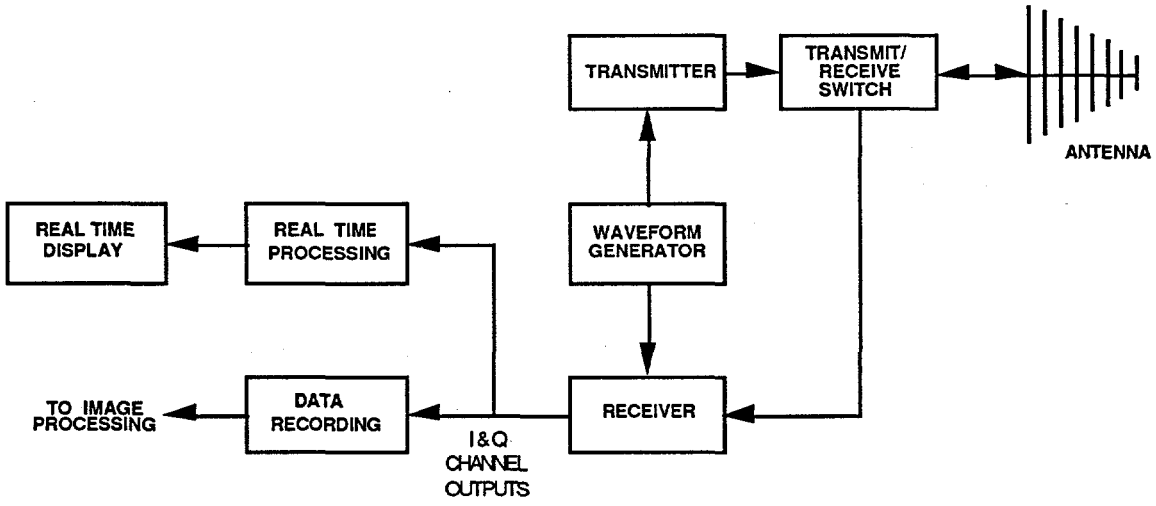

Figure 2.4.1.2-1. Simplified block diagram of radar equipment.

2.4.2 Mirage Test Vehicle

The Mirage Test Vehicle (MTV) contains the radar as well as the data collection equipment. The MTV is a Mirage-owned capital asset, and is equipped to support projects in the field, such as the 3-D SISAR. The radar is mounted on a trailer generally referred to as the Mirage Test Vehicle (MTV). The trailer allows the desired mobility for synthetic aperture testing while supporting the radar and

antenna on a pneumatic telescoping mast above the MTV. The telescoping mast allows convenient stowage for transport. The MTV has a gasoline powered generator and several 19-inch equipment racks for mounting various electronic support equipment. The MTV also has an operator console, Figure 2.4.2-1, based on a UNIX workstation for radar control and monitoring.

The original concept had all the equipment mounted in the MTV as a self-contained data collection and processing system. During the image processing development, it was realized that locating the workstation in the MTV resulted in an inefficient situation for software development and processing of collected data. Having the workstation located within the Mirage Systems facility results in a much more productive environment for software development and for image processing. Depending on the complexity of the image and its size, the computer processing can take from several hours to a day or more to process a complete image data set. In addition, the workstation does not have access to other resources within Mirage Systems when it is not connected to Mirage's computer network. Thus, it was determined that a much more satisfactory solution for development work is to keep the workstation in the Mirage lab and transfer radar data files via an 8 millimeter tape to the workstation, as shown in the lower portion of the system block diagram, Figure 2.4-3.

2.4.3 Software Architecture

Software programs were developed under this contract for radar control, data processing, motion compensation, matched filtering, and image display. Figure 2.4.3-1 illustrates the structure of the principle computer software configuration items (CSCI's). Each of these CSCI's are major development efforts and sets of complete documentation for them (program abstracts, logic manuals, user's manuals, installation guides, and annotated source code listings) are found in Appendices III - V. This document contains a description of the algorithmic approaches to promote an overall understanding of the operation and performance of the system.

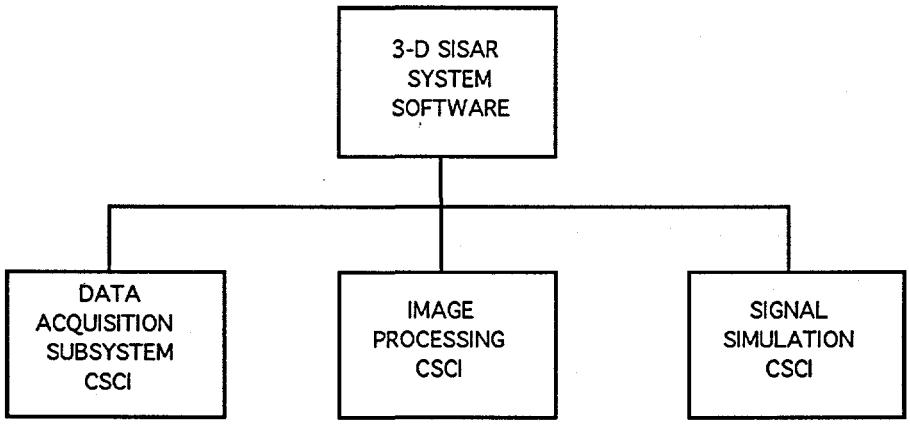

Figure 2.4.3-1. 3-D SISAR system software architecture.

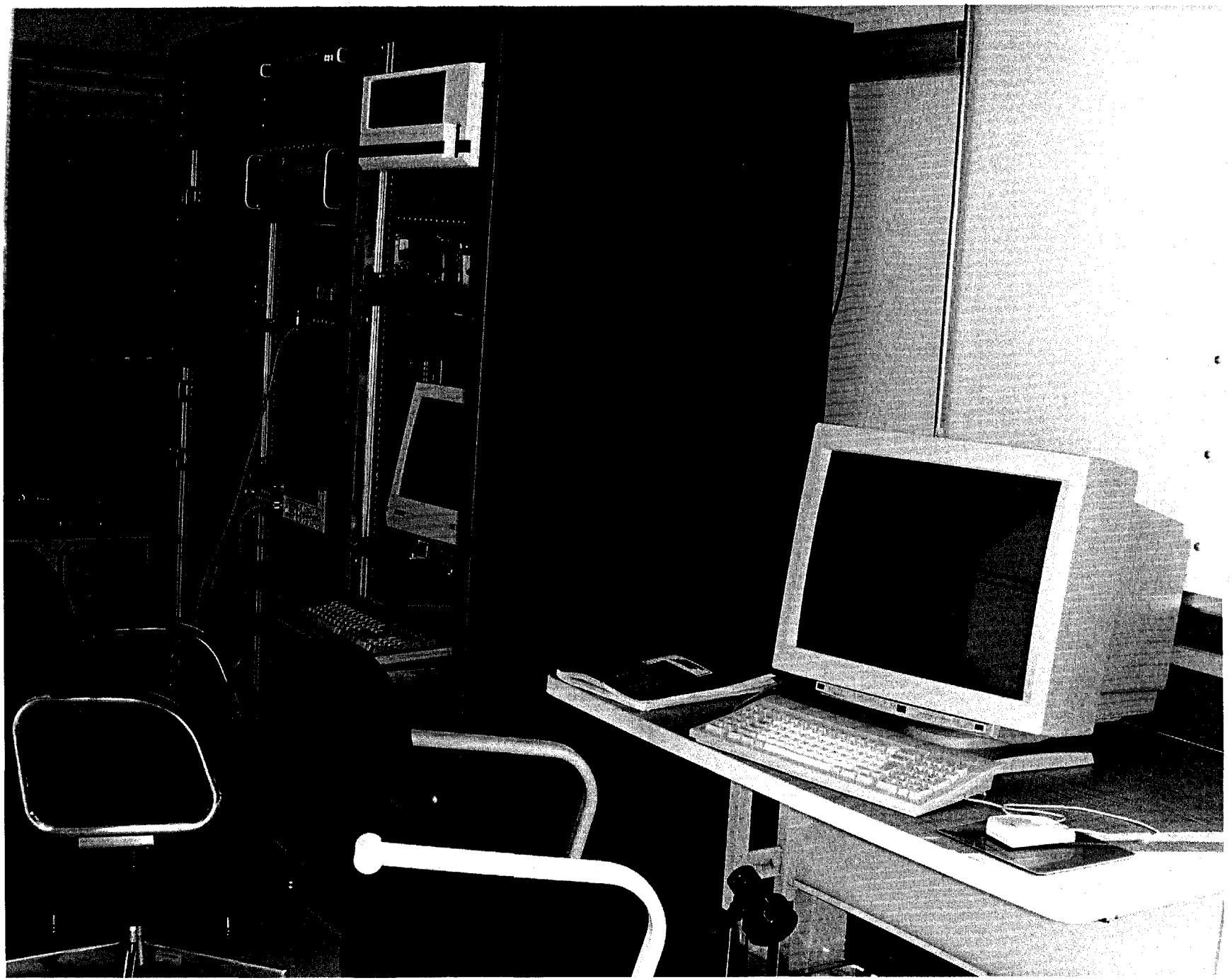

Figure 2.4.2-1. Radar operator's console and rack-mounted data collection equipment.

2.5 Radar Position Location

Mirage uses a set of three radar signal repeaters, Figure 2.5-1, in order to determine the location of the radar sensor during the site data collection process. The Motion Compensation algorithm produces an estimate of the location of the radar antenna in space for each radar chirp, and corrects the data for deviations of the antenna path from a perfect circle during data collection. The tip of the antenna, which is also the antenna feedpoint, is taken as the reference point for the antenna location, since it is easy to measure. The data input to the motion compensation program has previously undergone correction for the dispersive characteristics of the antenna which produce a variation of the electrical phase center of the antenna relative to its tip as a function of frequency.

The locations of the three repeaters are known with respect to the imaged volume. The motion compensation algorithm provides X, Y, and Z coordinates for the antenna with respect to the repeater locations for each chirp. These coordinates are calculated from the known spacings of the repeaters and the estimated ranges to each repeater. Each repeater produces an individually modulated replica of the incoming signal for retransmission to the radar. The individual modulations allow simultaneous measurement of the three distinct ranges. The modulations are also distinct from the normal buried object data and therefore do not interfere with the imaging data. The modulations also cause the repeater responses to appear at clutter free ranges permitting easier detection of the repeater signals. This process is described in Para 2.6.2.

2.6 Imaging Technique

The 3-D SISAR image processing technique takes the data measured by the radar and produces a map of the underground spotlighted region. The overall flow of this process is shown in the block diagram of Figure 2.6-1. Paragraphs 2.6.1 through 2.6.8 refer to the blocks of this figure. The following discussion provides an overview of the imaging process.. These processes are described in detail in Appendix III.

Initially, the data is corrected to remove any effects that the radar system itself may have on both the transmitted and received signal. The motion compensation software then uses the corrected data to determine the radar position at the beginning of each chirp. The 3-D SISAR data, along with the radar position, are used in the phase conjugate matching process to locate and identify all objects within the spotlighted region. This final step is an iterative process, where the predicted radar response due to various configurations is computed and then compared to the actual radar data through the phase conjugate match function. "Quality factors" are then used to determine the degree of match.

Figure 2.5-1. Radar signal repeater for precision location subsystem.

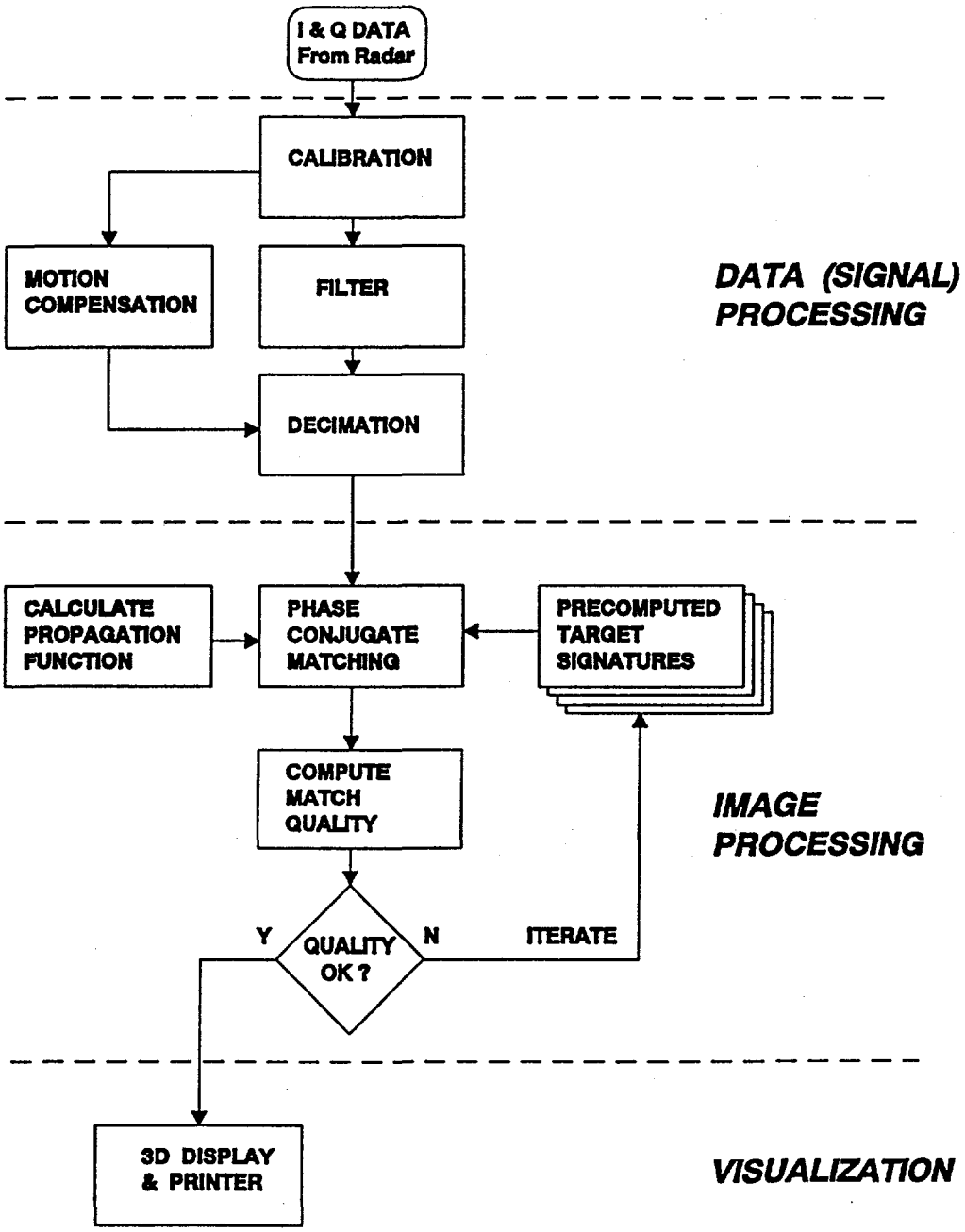

Figure 2.6-1. Image processing steps and data flow.

2.6.1 Calibration Program

There are several non-ideal aspects of the actual radar hardware. The calibration process modifies the data to correct for the effects of deviations in the system amplitude and phase response as a function of frequency. The performance of the radar components has been carefully measured to quantify these effects.

For instance, the radar amplitude is not perfectly flat over the 20 to 1000 MHz range due to variations in transmitter power, transmission line losses, antenna gain, etc. The phase center of the antenna is frequency dependent. The log periodic dipole array type antenna has a vee shape, and is fed at the apex by a transmission line from the radar. The highest frequencies are radiated from the apex region while the lowest frequencies are radiated from the rear of the antenna about 15 feet farther from the buried object. This increases the apparent electrical range of buried objects at low frequencies because the energy from the radar must travel an additional distance through the antenna structure and a similar distance through space for the lowest frequencies as compared to the highest frequencies. This happens twice, once while transmitting and again while receiving. The time delay in the radar signal created by this distance variation is spread out, or dispersed, over the radar operating frequency bandwidth.

Additional dispersive effects occur in the radar unit and in the antenna feed cable. These effects are much smaller than the antenna phase center effects but are also included. The calibration program corrects both the I and Q data values for these known amplitude and time delay non-linearities. Outputs from the calibration process are provided to the motion compensation and filter programs.

2.6.2 Motion Compensation

The imaging algorithm requires data which can be coherently processed. To achieve this, a phase correction is performed on the data for each chirp to account for any deviation of the antenna position from an ideal circular path. In the real world, the radar platform is not driven at a constant speed in a precise circular path, and the antenna is subjected to platform motion, vibration, and wind. Motion Compensation software estimates the position of the antenna so that a phase correction can be computed and applied to the data.

The Motion Compensation algorithm estimates the ranges to the three reference repeaters and solves a set of non-linear equations to produce an estimate of the x,y,z coordinates of the antenna. The repeaters are placed on the ground at the boundary of the illuminated volume containing the objects to be imaged, as was shown in Figure 2.4-1. It is assumed that the relative coordinates of each repeater have been measured at the time the radar data was taken and are supplied to the Motion Compensation algorithm. The range estimation process, shown in Figure 2.6.2-1, is performed on a set of collected

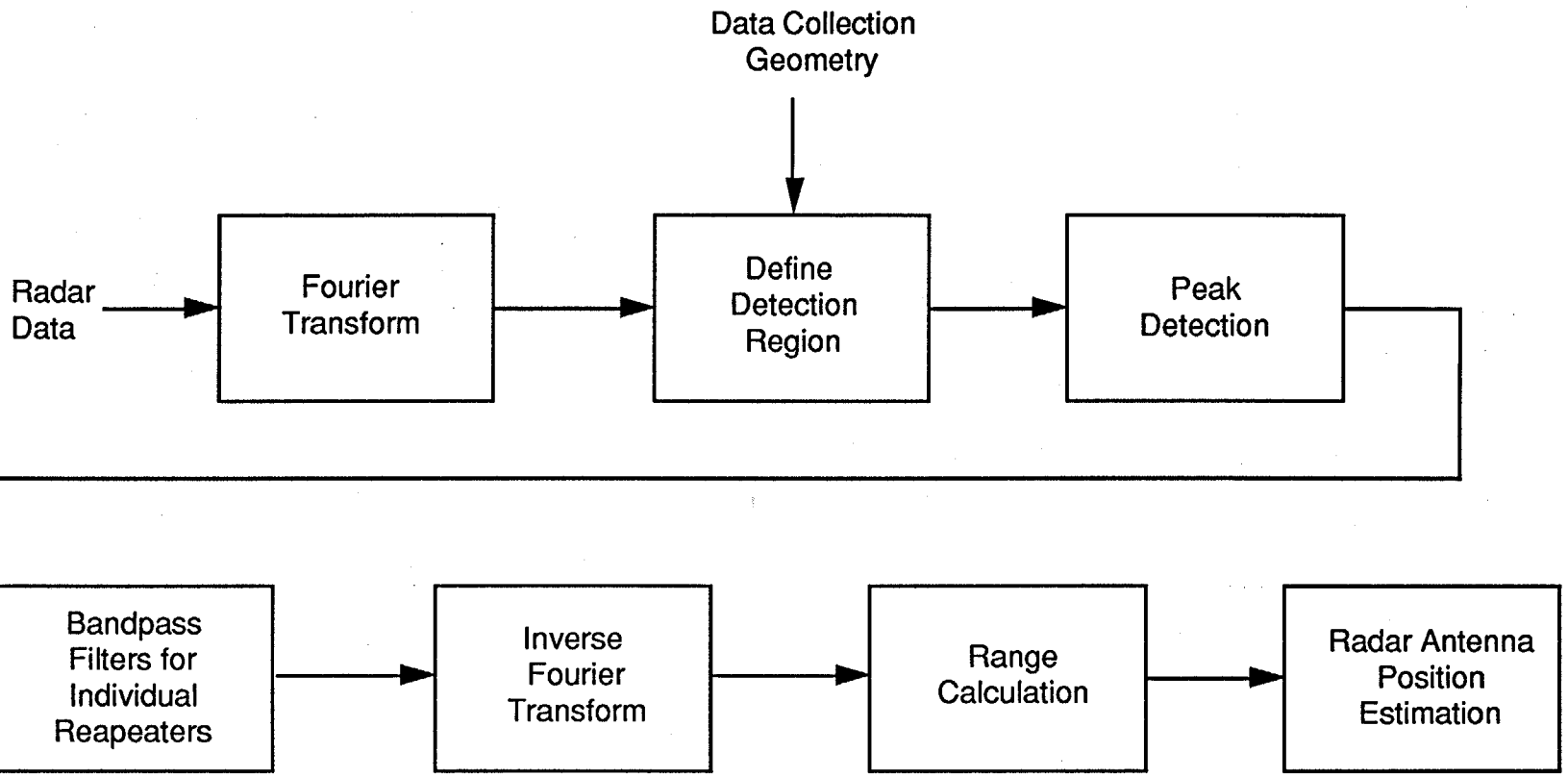

Figure 2.6.2-1. Repeater ranging and radar position estimation process.

radar data corresponding to each sweep in frequency (chirp), resulting in a position estimate for each chirp.

The repeater echoes will appear as narrow pulses in the FFT of the I and Q data of a chirp. The FFT bin containing the peak value of the pulse corresponds to a coarse range estimate of the exact range of repeater to the radar antenna. The FFT data is partitioned into "positive" and "negative" range bins. Objects and principal clutter will appear in the positive range bins.

The repeater differs from an ordinary object in that it reradiates a modulated form of the incident waveform in addition to its normal reflection. The frequency modulation creates duplicates (harmonics) of the repeater signal as viewed in the FFT response at bins away from and symmetrical about the base bin; the base bin corresponds to the actual range to the repeater. Use of an anti-aliasing filter and a sufficiently large modulation frequency results in only a few harmonic pairs. The purpose of using a modulated reference is to generate large responses in bins away from high object and clutter responses; this permits the use of simple peak detection schemes to find the response in a more benign signal-to-clutter region of the radar data spectrum. A different modulation frequency per repeater allows the differentiation of each repeater response from other repeater responses. Note that the repeater circuitry imposes a slight delay on the incoming waveform. The delay is computed from a separate measurement by comparing a repeater response to a flat plate response when each object is placed at the same location. The difference in range provides the repeater delay. This is then applied to all data sets to identify the set of bins through which the repeater response will traverse during a complete measurement set of all chirps.

Peak detection is applied to the FFT output to determine the peak bin. A bandpass filter is applied around each repeater's peak bin to produce an IQ data set for each repeater. Each data set now approximates a single tone data set. The single tone estimator is then applied to each successive IQ data set to produce an estimate of range to each repeater.

A single tone maximum likelihood estimator has been adapted to solve this multi-tone parameter estimation problem. The single tone estimator is generated by computing the phase differences between each successive pair of samples of a new IQ data set. These are then weighted and summed to form the range estimator. The result is a range estimate, $\hat{r}$, for each repeater according to:

$$\hat{r} = \frac{K}{2\pi} \sum_{m=1}^{M-1} wt(m) * \tan^{-1}\left(I\widetilde{Q}_m^* * I\widetilde{Q}_m\right)$$

where

$$wt(m) = \frac{1.5*M}{M^2-1}\left\{1-\left[(m-1) - \frac{\frac{M}{2} - 1}{\frac{M}{2}}\right]^2\right\}$$

and

$\tilde{IQ}$ = complex IQ data sample vector
M = Total IQ samples
K= fs/[(B/T)(2/c)] = conversion from normalized frequency to range
fs = sample frequency in Hz, which is the number of A/D samples/sec
B/T = chirp sweep range (B=chirp bandwidth, T=chirp duration time.
c = speed of light

The ranges to the three repeaters and the relative xyz coordinates of each repeater are sufficient to determine the location of the antenna during each chirp of the radar. The xyz coordinates are computed by solving a set of nonlinear equations presented in the Software Logic Manual found in Appendix III of this Report.

2.6.3 Filter Program

The I and Q data for each chirp contains both buried object and repeater information. A bandpass filter is used to remove information which does not directly contribute to the imaging process, and removes possible aliasing effects in the subsequent decimation process.

The repeater information is at greater ranges (higher frequencies) than true buried object data. The filter program removes the longer range repeater information from the I and Q data while preserving the true buried object information. Clutter from ranges which are too short to contain useful buried object information is also removed by the filter program.

2.6.4 Decimation Program

The decimation program reduces the amount of data to be processed by sampling a fraction of all frequencies in the I and Q data and by sampling a fraction of all azimuth angles as measured from the pit center. The radar collects more data than is really needed by the imaging algorithms although some of this additional data is needed for the precision required in range estimates for motion compensation. To process all of the data for image purposes would lead to very significantly increased processing requirements. For example, it is not uncommon to run preliminary analyses using only one fifth of all frequencies and one third of all angles.

In addition to reducing the number of frequencies and chirps represented in the data, the decimation program is responsible for associating an (X, Y, Z) location

of the antenna with each chirp of data in its output. The location data is received from the motion compensation program.

2.6.5 Propagation Function

The propagation of the signal from the radar to the buried object and return can be calculated for any buried object location. This is accomplished by breaking the propagation into several factors, each of which corresponds to a segment or event in the round trip propagation from radar to buried object and return.

Figure 2.6.5-1 shows the general pattern of propagation from the radar to the buried object. Radiation from the antenna will pass through the air to a point on the surface of the ground with energy losses due to spreading. For the short ranges involved with this radar this above ground propagation segment is treated as a spherical wave. When the signal strikes the air/ground interface it divides into two parts. Reflected energy travels away from the radar and is lost. The transmitted (refracted) portion of the signal energy passes into the ground with a change in propagation direction which depends on the complex dielectric constant (including the losses due to conductivity) of the ground. Further, the formerly spherical wavefront is distorted by the lossy media into a wavefront definable by two radii of curvature. The methods of geometric optics are used to calculate the propagation loss in the ground which depends on the distance traveled, the frequency and the complex dielectric constant.

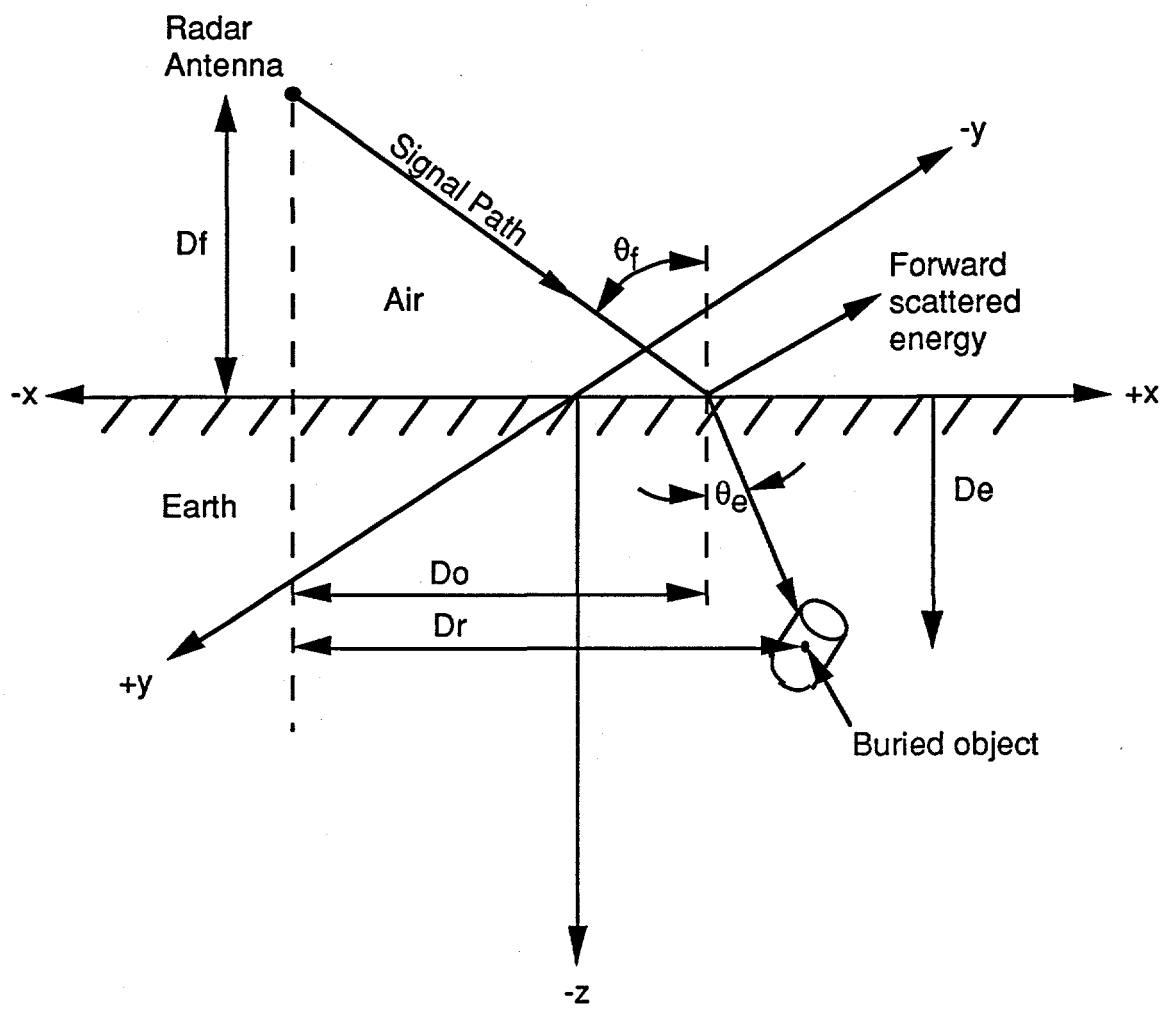

Figure 2.6.5-1. Radar signal propagation path.

The propagation calculations are designed to use a multi-layered model of the underground propagation media. This refinement is necessary because most real world soils differ in their electrical properties with depth due to different soil materials and/or different moisture contents.

After the signal reaches the buried object the energy is scattered. The scattering effects are modeled separately as discussed in the next paragraph. The scattered energy travels back to the radar along the same path it took toward the buried object experiencing similar losses although the details differ because the scattered energy leaving the buried object in the ground is assumed to have a spherical wavefront.

The propagation function depends on several variables as listed below:

- complex dielectric constant of the lossy ground (varies with frequency)
- different layers of ground with differing complex dielectric constants
- depth of assumed buried object

- radial horizontal distance from radar to buried object
- height of radar above ground
- frequency of operation

The true path length in each of the media is calculated by algorithms which determine the true geometric ray path of the energy by iterative means. The path length in each media component along with the complex dielectric constant in that media component and at each frequency used by the radar are used in the calculation of the overall propagation function.

To reduce computation time the propagation function is precalculated for a span of variables to generate a multidimensional reference table. During run time, the main imaging program uses interpolation between values in the table to establish the actual complex value of the propagation function.

2.6.6 Precomputed Buried Object Signatures

The radar is designed to detect a wide variety of underground buried objects. The approach used models the buried object signature (or scattering function, **S**) for the buried object type, size, and orientation and for various complex dielectric constants to characterize the lossy media in which the buried object is embedded. The buried object signature describes the reflectivity as a function of the two orthogonal measures of angles of incidence, the two orthogonal angles of the scattering and, of course, frequency.

The simplest type of buried object to be considered is a point scatterer. This type of buried object does not need to have an orientation angle because it scatters energy equally in all directions. Also, a point scatterer is achromatic in that its scattering is independent of frequency. Real world buried objects are generally more complicated in having spatial scattering patterns which vary in two angular dimensions and also vary with frequency.

For this program most buried objects are modeled as bodies of revolution although more complex buried objects can be modeled. This modeling is chosen in the interest of simplification and reducing the computational workload while providing an adequate model for many real buried objects of interest. Only one angle is needed to characterize the scattering pattern of a body of revolution while more complex buried objects require two angles to characterize their spatial scattering.

Buried object signatures are precomputed. A library of different buried objects and different orientations in different media has been prepared. Additional buried objects and orientations can readily be added. Each buried object signature is calculated in a form such that the overall propagation characteristic including buried object signature can be calculated as the product of the various components. This also allows a point buried object to be assumed by default in the absence of a specific buried object signature.

2.6.7 Image Formation

Image formation is the central program and process in the processing of the radar data. The input data for this program consists of:

- calibrated, filtered and decimated radar I and Q data
- radar position at beginning of each chirp
- precomputed propagation function
- precomputed buried object signatures

In addition, the user must specify the imaging volume of interest in terms of the span in x, y and z dimensions as well as the desired incremental resolution in each of these dimensions. Also, the user must specify a buried object or list of precomputed buried objects and orientations for which the image program should search.

The buried object space below ground can be subdivided in each of the three dimensions into voxels which are the three dimensional equivalent of pixels. For each voxel, a propagation function can be calculated which defines the magnitude of the radar return signal for a unit buried object located at that voxel. If the buried object is a true point buried object which scatters energy uniformly in all directions, it's scattering function can be taken as unity. However, for most real buried objects where their dimensions are not negligible with respect to a wavelength in the media at the highest frequencies used, a scattering function must be calculated which defines the scattering at the angles of interest. This scattering function, Φ, is defined as

$$\Phi = \tau_{ef}\tau_{fe}\, S\, \frac{e^{-2k_o.D_e} \bullet e^{-2jk_o n_f^{eff} D_f \sin\theta_f} \bullet e^{-jk_o(n_r^{eff} D_e + D_f \cos\theta_f)}}{D_f^2 + D_o^2} \bullet \frac{\cos\theta_f}{\cos\theta_e \bullet n_r^{eff}}$$

where

τ_{fe} = the transmission coefficient from the air into the ground

τ_{ef} = the transmission coefficient from the ground into the air

S = the scattering function that represents the signal change due to scattering from the buried object

$k_o = 2\pi/\lambda$

n_f^{eff} = (defined below)

n_r^{eff} = (defined below)

D_e = depth of the object

D_r = horizontal distance from the radar to the object

D_f = height of the radar above ground

D_o = horizontal distance that the signal travels in the air

θ_e = the angle of propagation in the ground

θ_f = the angle of incidence onto the ground

with

$$(n_r^{eff})^2 = \frac{1}{2}\left[\varepsilon_r - \sin^2\theta_f + \sqrt{(\varepsilon_r - \sin^2\theta_f) + \varepsilon_i^2}\,\right]$$

and

$$(n_f^{eff})^2 = \frac{1}{2}\left[-(\varepsilon_r - \sin^2\theta_f) + \sqrt{(\varepsilon_r - \sin^2\theta_f) + \varepsilon_i^2}\,\right]$$

Figure 2.6.5-1 shows the geometric relationship between these quantities. Appendix III contains the full derivation of the above equation.

To search for the existence of a buried object in the 3-D volume of interest, the image processing is done separately for each voxel. For each voxel the expected radar return for a point scatterer at that voxel location is calculated. This ideal radar return is compared to the actual radar return in a correlation process. If no buried object is present at that voxel location the result of the correlation process will be a small random number. If an actual point scatterer were present at that location, the correlation is a large number. Thus, each voxel will have a number which can be correlated with the likelihood that the expected buried object is present at that location.

The correlation process is actually a matched filter involving a double summation of correlation products which compare the actual radar output with the expected output for a buried object at that location for all frequencies in the radar coverage and for all azimuth angles of the radar with respect to the buried object volume. Thus, the correlation process involves many (typically about 1000) azimuth angles and many (typically several hundred) frequencies, each of which has a correlation calculation made and summed into a grand total for that voxel. This process can be expressed as:

$$g(x, y, z) = \frac{\sum_{f,\phi} G(f,\phi)\Phi(\text{object}, \varepsilon, x, y, z, f, \phi)}{\sum_{f,\phi} \left|\Phi(\text{object}, \varepsilon, x, y, z, f, \phi)\right|^2}$$

where

$g(x, y, z)$ = the correlation function

$G(f,\phi)$ = the radar data as a function of frequency and angular position

Φ = the expected scattering response of the buried object

f = frequency of the radar for each data sample

ϕ = angular position of the radar for each data sample

$\mathcal{E}$ = the complex dielectric constant of the soil, $(\varepsilon_i + \varepsilon_r)$

(x, y, z) = position of the center of the object

object = the type and orientation of buried object

When $(x, y, z) = (x_o, y_o, z_o)$, the location of the center of the buried object, $g(x, y, z) = 1$ for the ideal case, indicating a perfect match. Appendix A of the Imaging Logic Manual contains a complete derivation and description of this process. Figures 2.6.7-1 through 2.6.7-5 illustrate how the correlation function behaves with depth for an object buried at 4 meters. These plots were produced using the Radar Data Simulator described in Appendix V.

The initial search of a buried object volume for buried object returns is usually made using a point scatterer buried object model and large voxels for quick calculations. This often suffices to detect the presence of buried objects and determine their approximate locations. More accurate location and identification of buried objects can then be made using the precalculated buried object signatures (scattering functions) which are processed using a matched filter approach and finer grained voxel spacings.

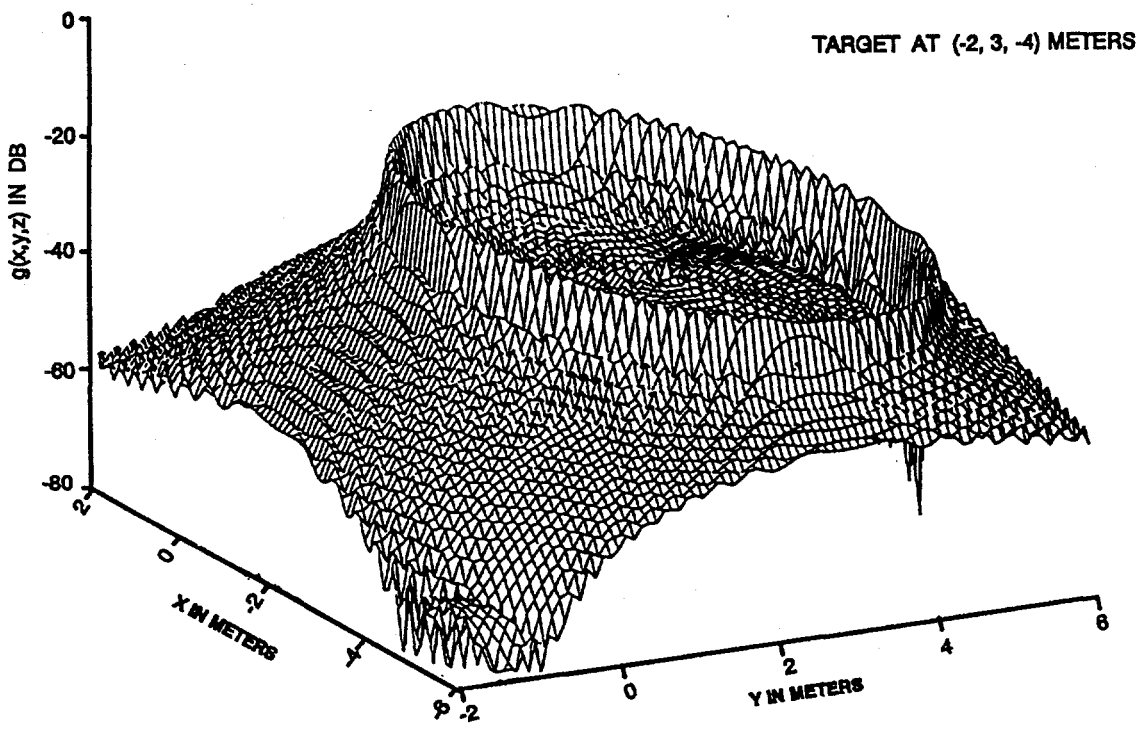

Figure 2.6.7-1. Matched filter output calculated for depth slice at 2 meters

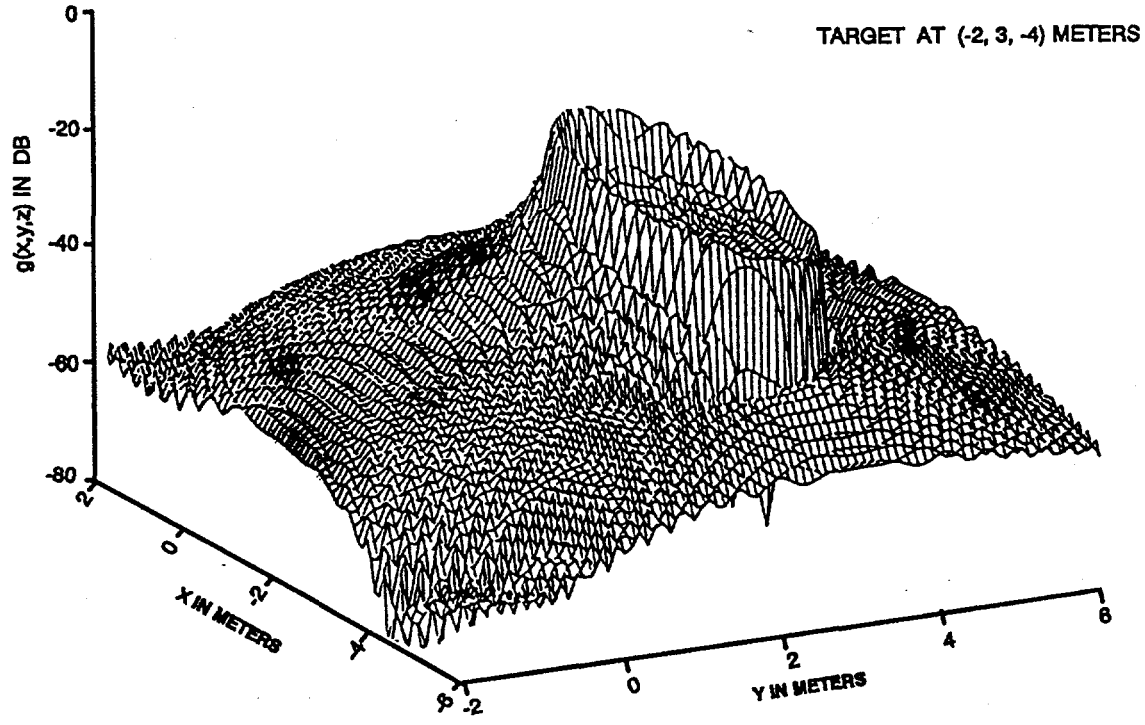

Figure 2.6.7-2. Matched filter output calculated for depth slice at 3 meters

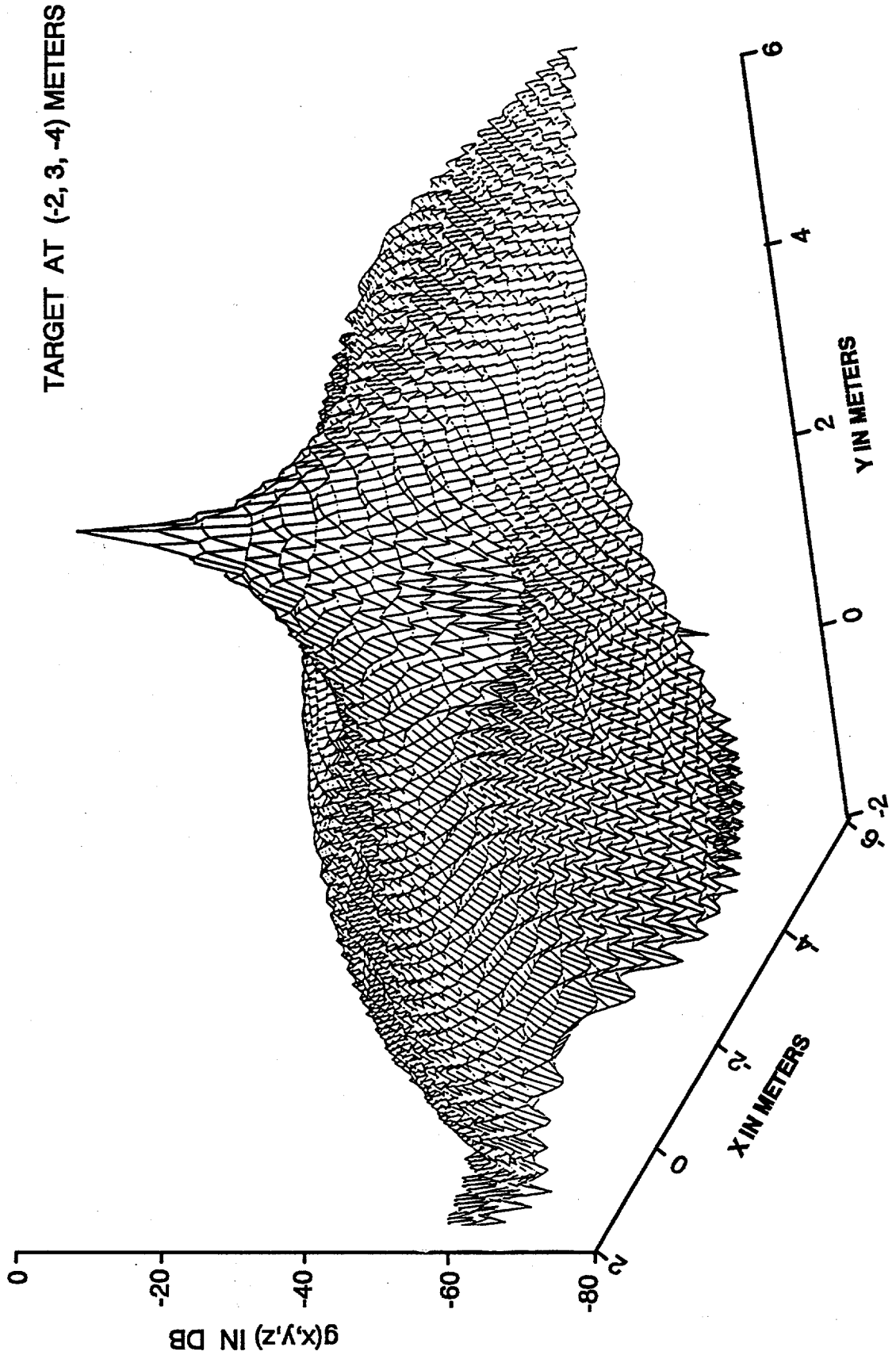

Figure 2.6.7-3. Matched filter output calculated for depth slice at 4 meters

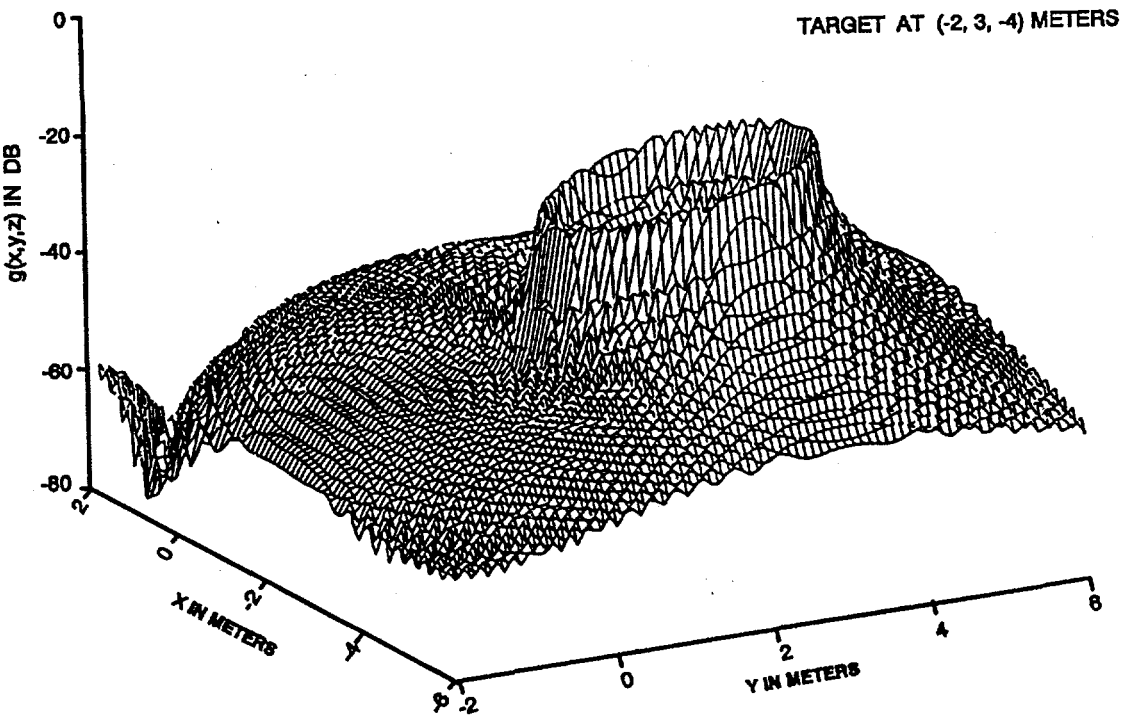

Figure 2.6.7-4. Matched filter output calculated for depth slice at 5 meters

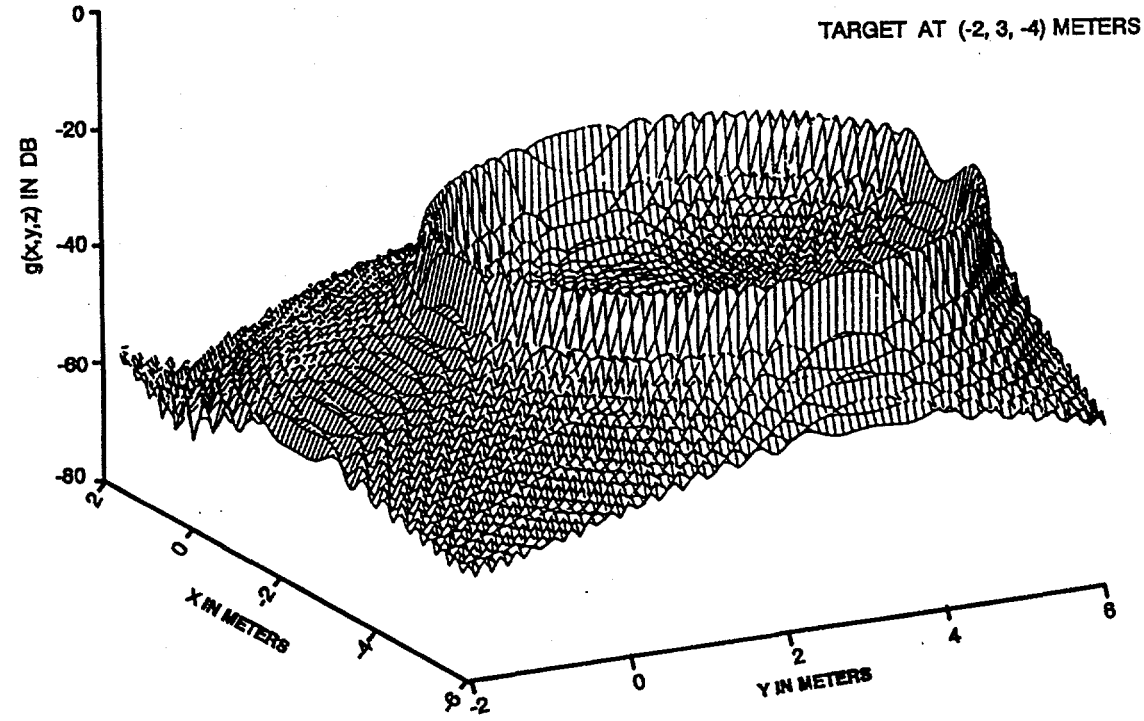

Figure 2.6.7-5. Matched filter output calculated for depth slice at 6 meters

2.6.8 Match Quality

When using the matched filter process involving various types of buried objects and orientations it becomes necessary to compare the results for the different buried object signatures. This comparison is called Match Quality and is used to determine the relative effectiveness of the buried object matching results.

The matched filter process produces an output number which is proportional to the degree to which the actual radar output matched the particular expected output predicted for that type of buried object, size, and orientation at that location. When attempting to identify an unknown buried object, the procedure calculates the matched filter correlations for a series of buried object candidates. These candidates are then ranked in terms of their overall correlation with the received signals.

The measure of the quality of the match, Q_p, is defined as

$$Q_p = SNR + 10*\log(G_p/V_p)$$

where

SNR = the ratio of the average value of the matching function, g(x, y, z), within the peak region and the average value of g(x, y, z) outside the peak region, in dB.

G_p = the "correlation factor", which is equal to the maximum value of g(x, y, z).

V_p = the volume of the peak region, in m^3. The peak region is defined by the region around (x_0, y_0, z_0), the location of the maximum of the matching function, within which g(x, y, z) exceeds $0.25G_p$.

The quality match recognizes a set of quality factors for each buried object. Larger values of Q_p correspond with better matches. Good matches have a high peak value, high SNR, and a small volume around the peak. Low ranking buried objects are eliminated. If several buried objects show high quality matching, the user must either accept the highest quality match as the identified buried object and location or zoom in to the highest quality match region and make more detailed analyses including further comparison of the higher ranked buried object types, sizes, and locations. The technique is covered fully in the Appendices to the Imaging Logic Manual.

There is always a tradeoff between the resolution of correlation function and processing time. Coarser resolutions are appropriate for a "quick look" analysis which is followed by a more focused and more detailed analysis. However, if the buried object location voxel size is too large, the matched filter correlation will be degraded, perhaps to a degree causing buried objects to be missed.

2.7 Test Program

The test program may be divided into four phases where the radar was tested in a variety of situations. These four phases are as follows:

- System Integration testing
- Stanford University field tests
- Shoreline Amphitheater field tests
- Mirage Test Site field tests

Computer data files were created for each of the formal tests. These data files have been archived for future use. Each such formal test has a one page form (both sides) on which pertinent data associated with that test is recorded. All data files are archived on 8mm tape cassettes in UNIX file format.

To date, 286 formal test files have been recorded, as summarized in the table below.

Table 2.7-1. Summary of 3-D SISAR test activities.

Location	Dates	Number of Files
Local Area	9/94-12/94	26
Stanford Test Site	12/94	46
Local Area	4/95-5/95	72
Shoreline	5/95	47
Shoreline	7/95	33
Mirage Test Site	7/95	36
Shoreline	8/95	26
Total		286

The local tests were perfromed in the Mirage Systems parking lot. The Stanford Test Site test data files were gathered at a site located on the main campus in two separate weeks in December 1994. The Shoreline tests were made in the parking lot of the local Shoreline Amphitheater where sufficient unobstructed room exists to gather data on above-ground objects while using the circular spotlight mode SAR geometry, as was used in gathering underground test data. The Mirage Test Site is a specially constructed pit filled with test objects as described in Section 2.3.4.

A test data file consists of nearly 3600 16-bit samples of the radar I and Q output channels for each chirp. For the typical 20 to 1000 MHz chirp span this provides samples at approximately 0.25 MHz intervals in frequency. Including the unused radar sweep flyback time prior to beginning a new linear chirp, 26.7 chirps per second are collected. Typically, the time used to circle the test area is 180 seconds, and includes about 4800 chirps. Therefore, each chirp accounts for about 0.075 degrees of azimuth.

2.7.1 System Integration Testing

Following completion of the various modules comprising the radar, integration tests were performed to measure the overall radar performance. These tests included sensitivity tests to determine the receiver noise figure and thereby establish the thermal noise levels which define receiver sensitivity.

Dynamic range tests were made to establish the instantaneous dynamic range which establishes the radars ability to detect weak signals while simultaneously receiving other strong signals such as ground clutter. It is important that the radar handle strong signals without having internal non-linearities generate spurious signals which could mask the desired weak signals from buried objects. These strong signals are often described as clutter and arise from such sources as the reflection of the transmitted signal from the ground surface and nearby objects.

It is important to the imaging algorithms that the overall transfer function be accurately known. The transfer function characterizes the overall amplitude and phase characteristics of the radar over the full frequency range. The transfer function is measured in three parts, the antenna characteristics, the antenna feed cable characteristics, and the overall characteristics of the radar unit as measured at the antenna port. This involves precise measurement of the antenna, including gain and phase characteristics over the full frequency range. The antenna feed cable was measured using a network analyzer. The radar itself is measured by using an attenuator and a long cable (50 feet or more) and an attenuator. The long cable is short circuited at the far end while the near end is connected to the radar through an attenuator. Transmitted energy from the radar passes through the attenuator and cable and is reflected at the far end. This reflected energy is detected by the radar receiver. The amplitude and phase characteristics of the cable and attenuator are then measured carefully on a network analyzer. From these data the overall radar transfer characteristic is calculated.

Additional tests conducted during system integration included measurements of test objects above ground, including a dihedral corner reflector with 4 foot by 4 foot facets, and reference metal spheres with diameters of 0.3 and 1.1 meters.

2.7.2 Testing at the Stanford University Test Site

Early in the program a search for test sites was conducted. Desirable site characteristics included the following:

Availability when needed
Flat, unobscured terrain
Simple support logistics and low support costs
Controlled environment
Favorable soil characteristics
Buried test objects of the types of interest to the DOE GPR program

These desirable characteristics led to the initial selection of a test site operated by the Department of Geophysics of Stanford University. This site is at the eastern edge of the Stanford campus only about 15 miles from MIrage and has objects of interest already buried at the site. The location avoided significant travel expense, was available and accessible with controlled access. There was minimal need for additional buried test objects and those already in place had known locations with an accuracy of nominally +/- 1 foot. The soil is loamy clay disturbed only to the degree necessary to emplace the test objects.

More than 50 individual formal tests were made including tests of the following types:

Calibrated sphere above and below ground
Data collection runs to quantify site clutter
RFI runs to assess interference from other environmental signals
Tests with and without cooling fans on
Tests with different repeater location geometry
Tests with static calibration runs appended
Tests with different radar data collection geometry's
Repeats of T&I noise figure and cable calibration tests.
Specific runs to detect buried objects
Faster and slower circles of test area with radar
Specific runs to detect buried assortment of drum lids and rings

Most of these runs resulted in data files of the order of 50 to 200 megabytes which were brought back to Mirage for detailed analysis.

The Stanford tests were completed in December, 1994. The next 3 months or so were devoted to analyzing the data and to designing a fix for a major deficiency discovered during the data analysis. This major deficiency was that the accuracy achievable by the motion compensation subsystem was inadequate due to low signal strength from the passive position location repeaters. This was ultimately corrected by a major redesign of the repeaters. The newer design uses amplification of the radar signal, and provide about 100 times greater output signal power. Interest in the Stanford test site decreased due to suspected strong nearby transmitters which aggravated the general urban RFI environment, and the fact that heavy winter and spring rains had

made the site a muddy morass, all but precluding any useful work until onset of the dry season. Another factor diminishing interest in Stanford test site was that the electrical characteristics of the soil were not well known and were suspected to be less homogenous than might be desired for the initial radar performance characterization. Thus, it was decided to construct a new test site to provide a more controlled and homogenous test environment.

2.7.3 Shoreline Amphitheater Tests

In the spring of 1995, a series of tests were made to carefully characterize the radar. These tests included 66 formal tests at Mirage primarily concerned with detailed analysis of the new active repeaters as well as additional baseline data concerning RFI from radio transmitters in the local environment. Also, during this period, a large turntable device called the "Whirlybird" was designed and fabricated. The whirlybird supported one or more active repeaters positioned in a geometry comparable to that normally used by the 3-D SISAR. The whirlybird was intended to simulate the motion (inverse) normally observed by the 3-D SISAR, and could be used in the more limited space of the parking lot at Mirage Systems. This allowed a convenient test of the redesigned position location repeaters and motion compensation software.

A series of above-ground tests were begun in late May, 1995 and continued for about a two month period. These tests were conducted in a large relatively uncluttered paved parking lot at Shoreline Amphitheater. The important aspects of this site were that it was nearly free of obstructions, local (about 4 miles away), and readily available. Because it was paved, no objects could be buried at this site. More than 80 formal tests were conducted, including the following:

Active repeaters at various ranges
Active repeaters with various modulation signatures
Tests of the capability to subtract clutter from the radar output
Tests using a dihedral corner reflector with 4 foot square facets
Additional tests of the whirlybird spinning repeaters.
Tests with and without a large calibration sphere
A suite of 11 tests to calibrate overall radar performance.

2.7.4 Mirage Test Site Tests

In order to have the flexibility to perform tests with more carefully controlled test conditions and object emplacement, Mirage constructed a test pit meeting these objectives. This pit was constructed to provide a known soil environment 8 feet deep having objects buried at precise locations. The test site is located 3 miles Northwest of Jamestown, CA which is about 100 miles east of San Francisco. The test site is a circular pit filled with sand to provide a homogenous underground environment. This allows easier characterization of the radar performance than possible with an arbitrary and uncharacterized medium. The sand also has better drainage than normal soil, thus reducing the variations in

moisture content which can have large effects on the propagation of the radio waves.

Figure 2.7.4-1 shows the general arrangement of the site. The test pit is about 8.5 meters in diameter at the surface and is about 2.5 meters deep with sides sloping at an angle of about 45 degrees. Figure 2.7.4-2 shows test objects being emplaced in the pit. The buried objects at the lower levels are considered permanent while the shallower levels are used for temporary buried object emplacements. For the tests conducted under this program the buried objects of interest include 55-gallon metal drums at the greater depths, and various pipes and other metal and dielectric buried objects distributed throughout.

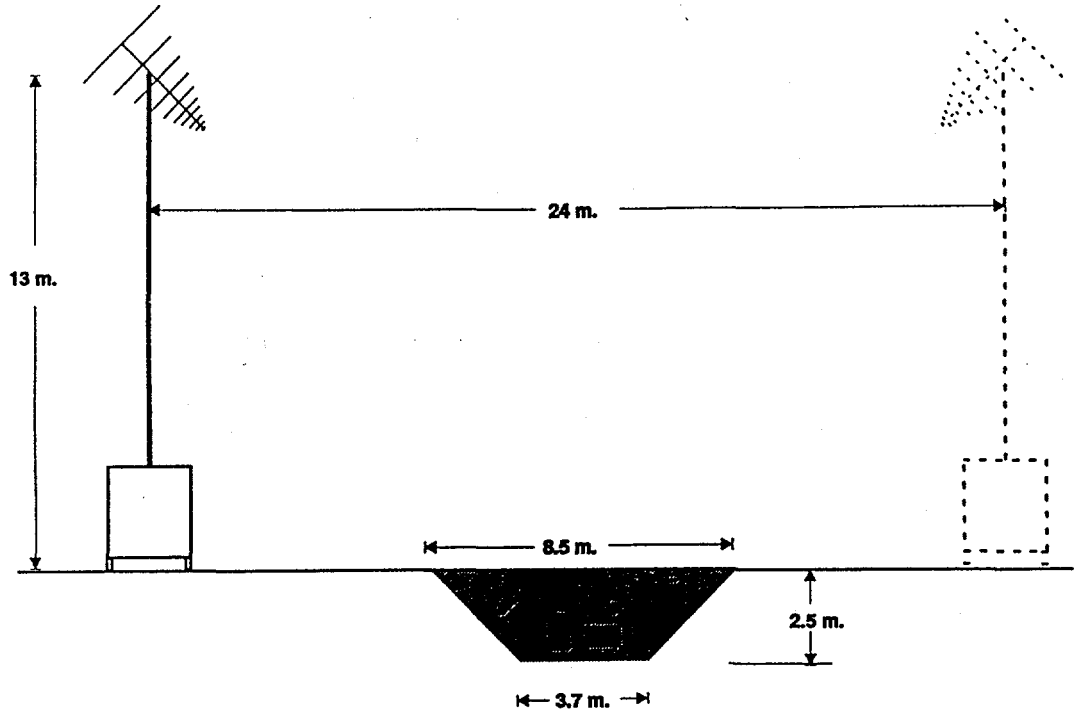

Figure 2.7.4-1. Arrangement of test site showing positioning of radar system and test pit.

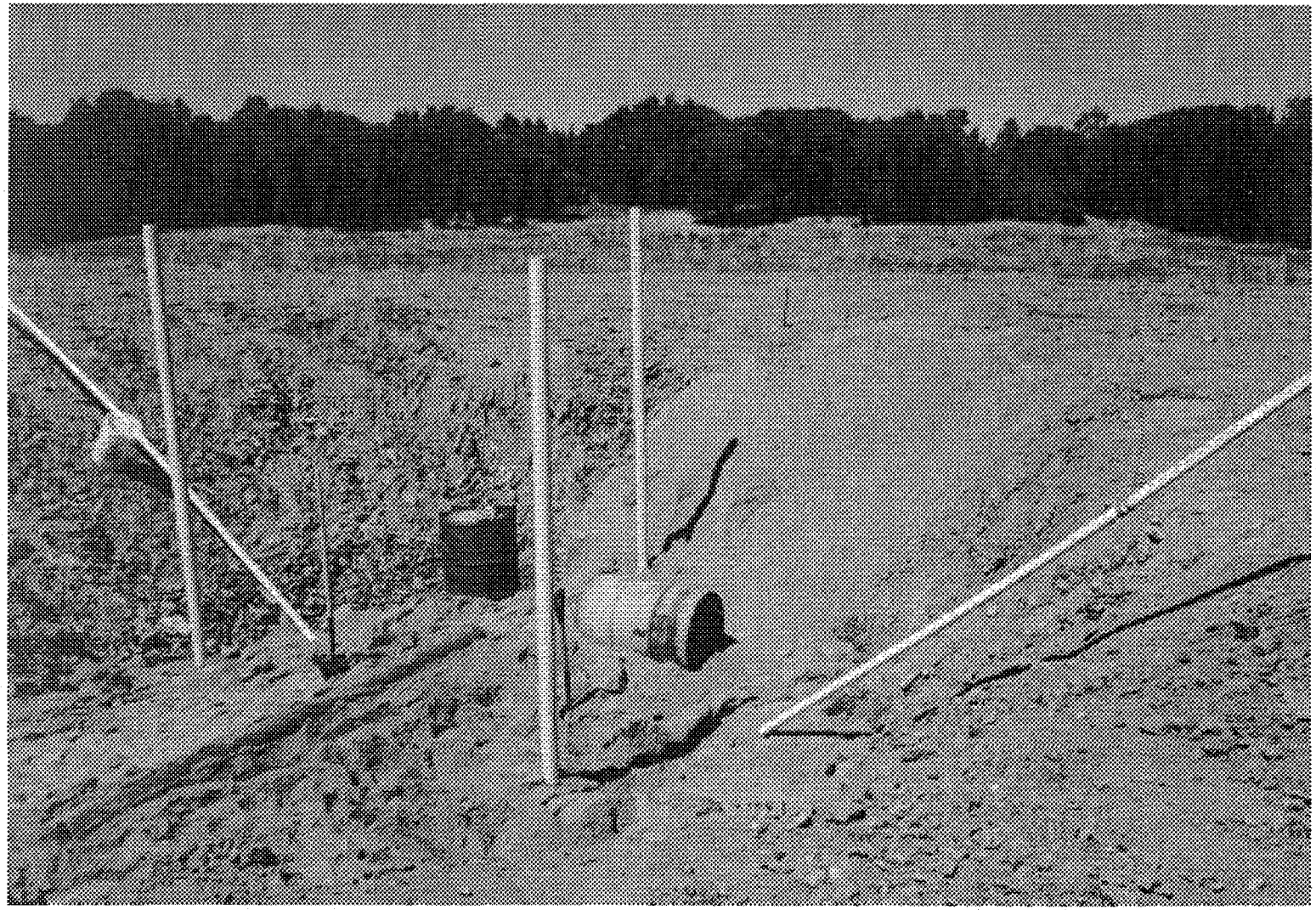

Figure 2.7.4-2. Objects being emplaced in Mirage test pit.

Permanent buried objects at deeper levels in the test pit include two 55-gallon metal drums, one lying horizontally and one vertically on end at depths of 7 feet to the bottom surface of each drum. A thick-walled section of 6-inch diameter metal pipe was placed near the bottom of the pit. A 12-inch diameter metal sphere was embedded at a depth of 3.5 feet. Various other metal and dielectric objects were placed at shallower depths.

Initial testing at the Mirage test site began in late July 1995. The first set of tests were the same as the set used at Shoreline, and were used to confirm that the radar continued to function as it had at Shoreline. Additional tests conducted at the test site included:

Repeaters ON and OFF
Small sphere above ground
Various frequency ranges chosen for possibly greater RFI immunity
Corner reflector tests at various ranges
Clutter reference files
Tests with differing receive attenuator settings

Sets of imaging data were collected under various operating conditions of the radar, and the processed results are shown in Paragraph 3.

3.0 Test Results and Discussion

The test data collected at the Shoreline Amphitheater and Mirage-built sites is still in the process of being evaluated and analyzed as of this writing. The data sets are being used to debug and refine the imaging algorithms, as the various phenomena involved with each step of the process becomes more clearly understood and applied. Therefore, the results presented here are considered interim results, showing the progress made at this step of what is seen as an evolutionary process. Progress in refining the imaging algorithms has been incremental, as the results of each experiment are investigated.

To date, images of several above-ground and below-ground objects have been processed. The images shown in this paragraph were all produced from test data taken at the Mirage-built test site described in Para 2.7.4. The program AVS 5 was used to display the imaging data. The image appearing in Figure 3.0-1 shows the detection and location of a 12-inch diameter spun aluminum sphere placed on the ground. The two red and one gray discs having a white vertical bar represent the locations of the position location repeaters placed on a circle on the test pit surface. The large white circular shape lying on the vertical axis shows the location of the sphere on the ground surface, and the red/yellow region slightly to the left of the sphere shows the location of the image produced from the test data. Since the sphere is not transparent, the sphere obscures part of the imaging data in this figure. For this particular measurement, the positional error is less than 0.1 meter in the X and Z axes, and about 0.1 meter along the Y axis.

The images appearing in Figures 3.0-2, 3.0-3, and 3.0-4 show the detection and location of two thin sections of right circular cylindrical metal test objects buried underground. The three large red circles having a small white circle in the center represent the position location repeaters placed on the test pit surface. The objects consist of a 12-inch diameter by 3-inch thick cylinder placed 12 inches underground, and a 6-inch diameter by 2-inch thick cylinder placed 6 inches underground. The smallest circle represents the location of a 3-inch diameter by 1-inch thick cylinder placed 3 inches underground. The test objects were placed on a line parallel to the X axis at Y = 1.8 meters from the center of the imaged area.

Data from the imaging algorithms appears as yellow shaded voxels within red circles drawn on the figure to represent the physical dimensions of the test objects. The location of the test objects on the figure are their actual physical locations during the data collection experiment. It can be seen from these figures that the imaging data portrays the correct location of the 12-inch and 6-inch cylinders, since the data falls within the diameter of the physical object in the X and Y dimensions, and is within 0.1 meter in the Z dimension. The 3-inch cylinder was not initially detected. In subsequent data analysis using higher resolution processing, the 3-inch cylindrical section was readily detected at the correct depth and location. The higher resolution processing employed voxel sizes on the order of size of the test object, 3x3x3 inches.

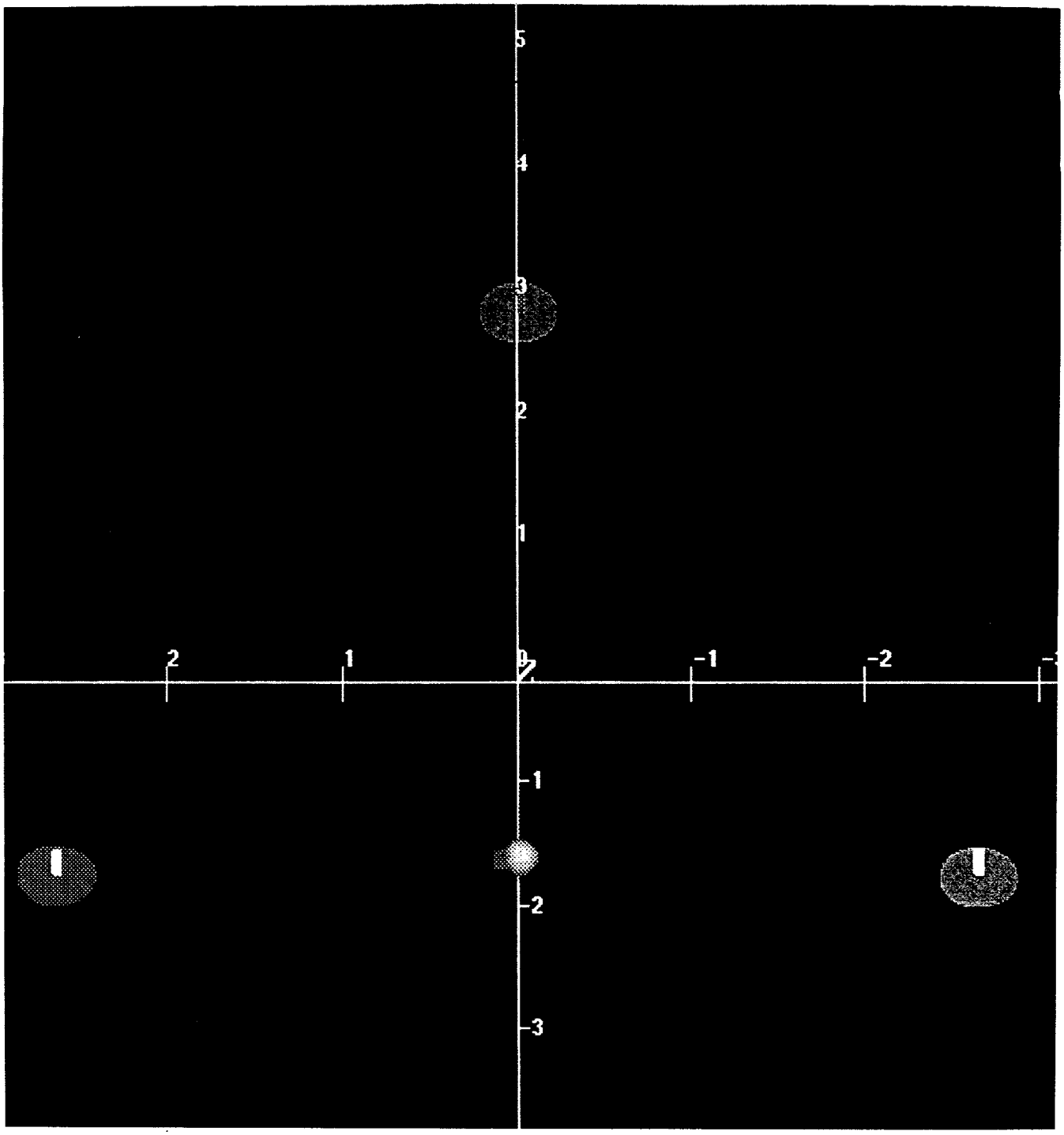

Figure 3.0-1. Image of a 12-inch metal sphere placed on the ground surface.

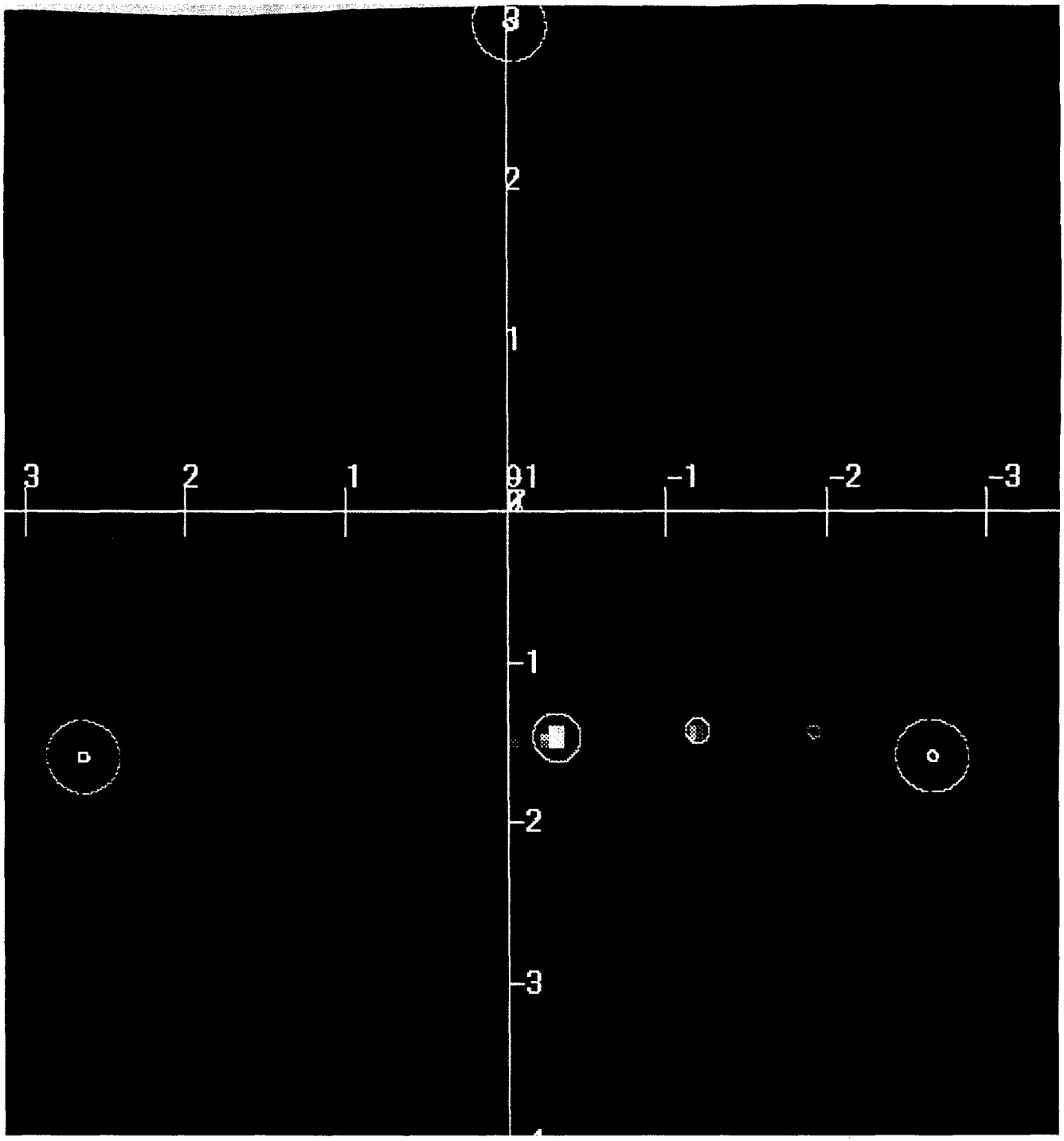

Figure 3.0-2. Image of several thin metal cylinders buried underground, plan view of surface of imaged area.

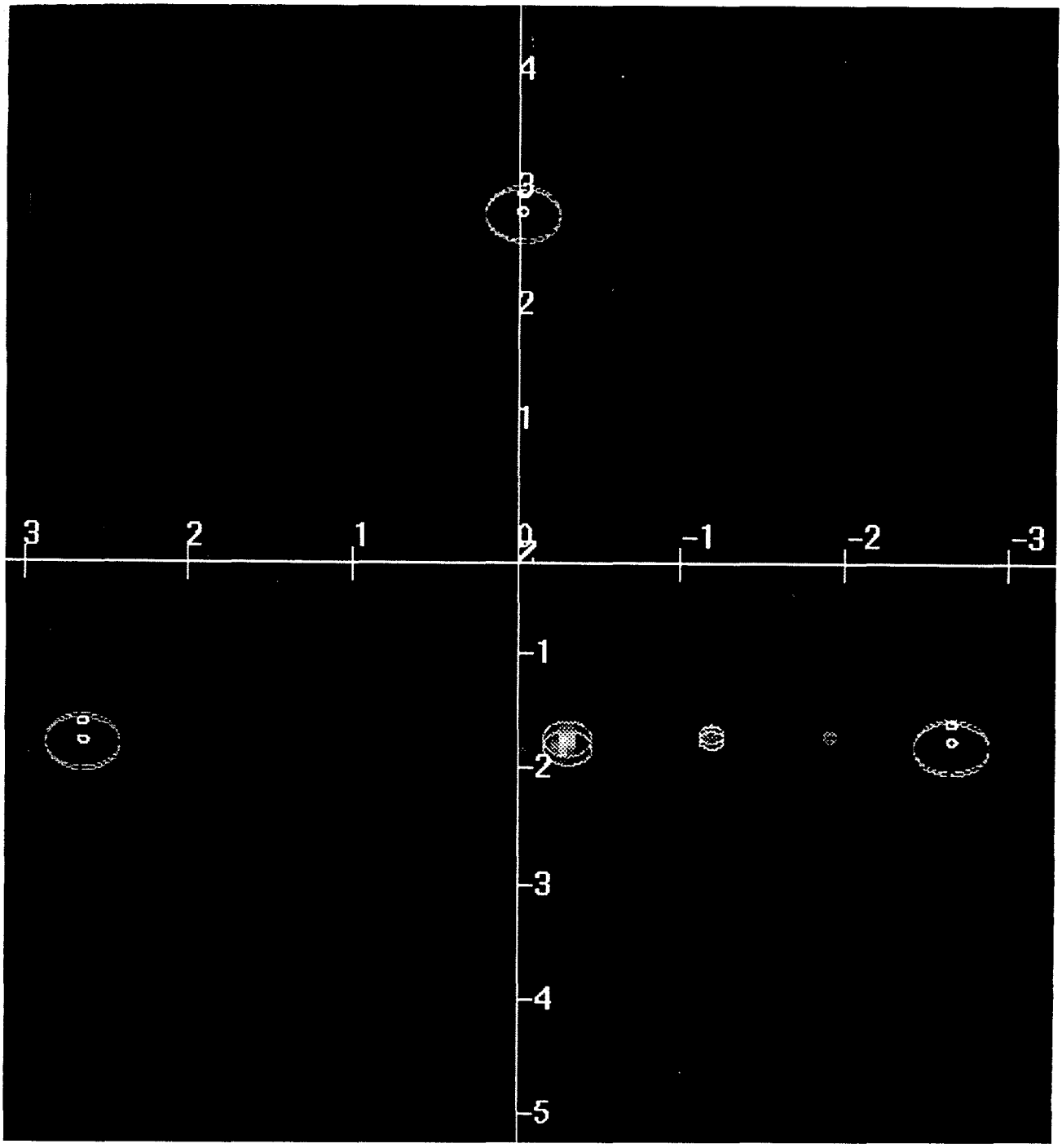

Figure 3.0-3. Image of several thin metal cylinders buried underground, with view of imaged area tilted by 45 degrees.

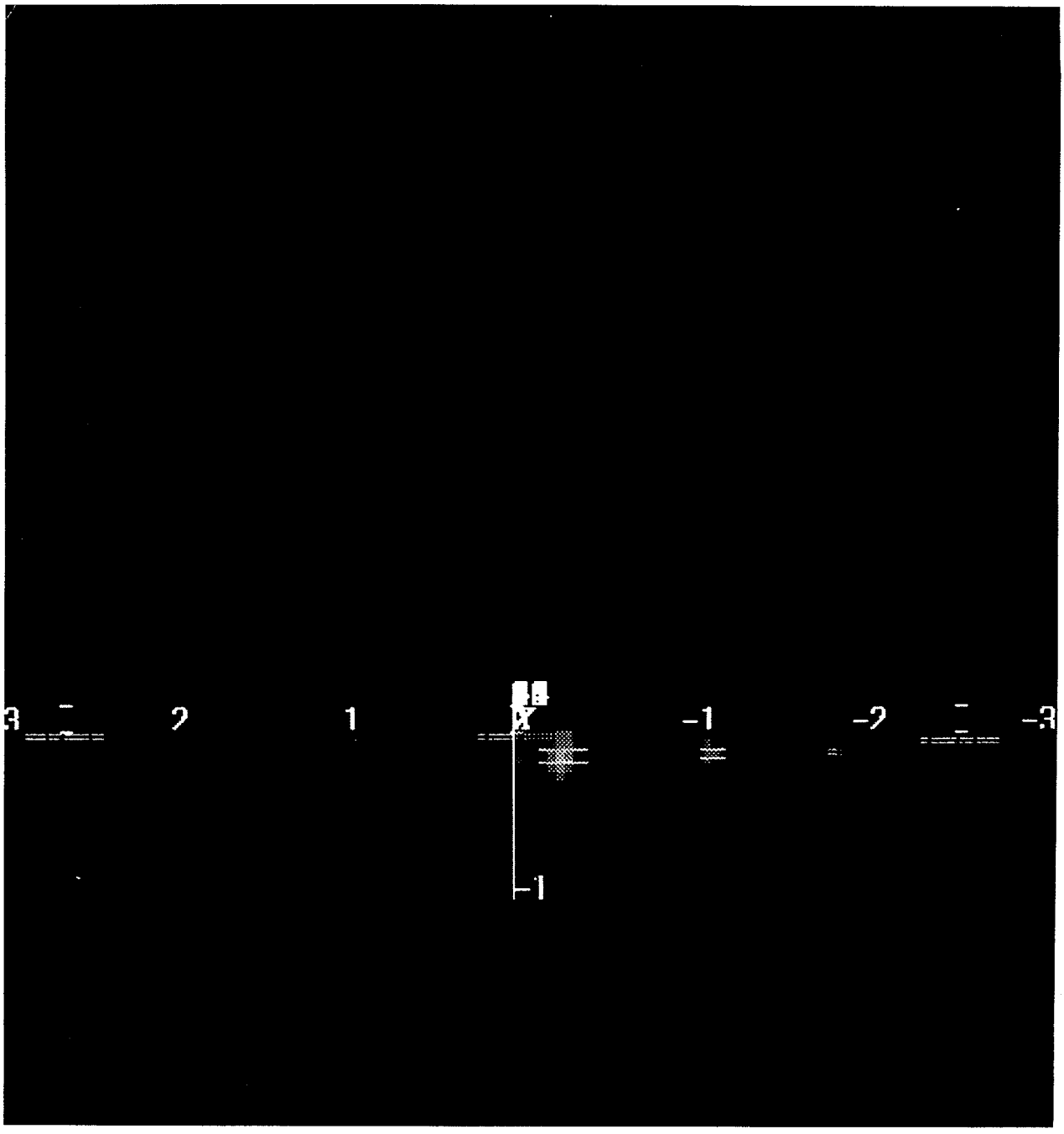

Figure 3.0-4. Image of several thin metal cylinders buried underground, with view of imaged area tilted by 90 degrees.

4.0 Conclusion

The major goal of this development effort is the remote detection, analysis, and mapping of buried waste containers from a mobile platform. From the testing and analysis performed to date, the 3-D SISAR has achieved the detection, accurate location, and three-dimensional imaging of buried test objects employing the stand-off SAR geometry. Tests have demonstrated that underground objects have been located to within 0.1 meter of their actual position.

This work validates that the key elements of the approach are performing as anticipated. The stand-off synthetic aperture radar (SAR) methodology has been demonstrated to be a feasible approach as a remote sensing technique. The radar sensor constructed under this project is providing adequate quality data for imaging, and the matched filters have been demonstrated to provide enhanced target detection. Additional work is on-going in the area of underground propagation and scattering phenomena to provide enhanced depth performance, as the current imaging results have been limited to a few feet of depth underground.

Due to the limited depth measuring performance obtained to date, no attempt has been yet made to detect and image plumes and pit boundaries. This effort should be included in the future testing of the radar, as the image processing capabilities continue to improve.

Improving the depth of imaging has several aspects. The on-going imaging algorithm improvements mentioned previously are expected to yield significant improvements in the depth performance in the near future. The depth performance of the radar may possibly be improved by a more complete exploration of the effects of the low frequency portion of the radar frequency chirp. The lower portions of the frequency spectrum penetrate the earth much more readily than the higher frequencies, and are likely to be the primary mechanism for achieving the goal of imaging to a depth of 10 meters.

For much of the imaging work, the frequencies below the region of 150 MHz were not found to significantly contribute to the imaging performance and image quality. This was due to factors inherent in the radar and the design of the experiments, and are primarily caused by the frequency dispersive characteristics of the large antenna structure. The antenna structure delays the propagation of the low-frequency portions of the sweep by upwards of a hundred nanoseconds. Since the test site dimensions were fairly small in order to keep construction costs reasonable, the dispersive time delay created by the antenna was an appreciable part of the propagation time to the buried objects. This prevented an optimum setting of the transmit-receive gating delays for the radar for the entire radar bandwidth. Since there is only one delay available, it was chosen to optimize the radar sensitivity in the region of the repeater signals, which are at the upper portion of the frequency range, deemphasizing the signals from the lower frequencies.

The second phenomena associated with the large antenna structure is the fact that it takes additional time for the transmitted signal energy to dissipate along the length of the structure. This means that, for short range operation, some residual energy may be present on the antenna during the receive portion of the transmit-receive cycle. This extraneous energy can obscure the desired signals reflected from the test objects in the low frequency region of the radar bandwidth. Both of these phenomena are significantly lessened by operating the radar with a larger data collection geometry, but none was available for the limited testing performed during this project. It is anticipated that the low frequency performance of the radar will undergo a more complete evaluation during the next testing phase.

5.0 Future Work

5.1 System Evaluation At A DoE Test Site

Comprehensive testing performed at a calibrated DoE test site (i.e. Rabbit Valley) would assess and establish GPR system performance in a realistic environment against underground objects specific to the interests of the DoE.

It is suggested, that for these consequential tests, certain system upgrades, based on lessons learned in the initial DoE program, be incorporated. The inclusion of these changes would significantly increase the system performance and value of the testing.

Following tests at a calibrated DoE test site (or test sites), the upgraded, fieldable prototype system could then be deployed to actual DoE waste sites to perform site characterization testing.

5.2 System Upgrades

Technological advances and innovations conceived while developing the 3-D SISAR could be adopted at low cost and with low risk. The major components of the system would be largely unchanged. The data processing and antenna portions of the system would benefit from upgrades.

While low frequency testing and evaluation was not extensively examined, it is believed that the lower frequencies did not substantially improve the images achieved. As such, a smaller antenna system could be adapted that would increase transportability and practical operation without a penalty in performance. This system modification lends itself to the feasibility of the contemplated platform migration described below.

Ways to reduce the processing time for the image formation algorithms are of interest. The direct approach is to purchase a faster computer. A more sophisticated approach would be to purchase a computer that is more structured to fit the form of the computational problem. Since the imaging

involves a considerable amount of matrix mathematics, an array processor should be of benefit. Even more effective would be the use of parallel processing techniques so that portions of the imaging could be computed in parallel. The optimum solution would require some investigation of the benefits and limitations of each approach.

Further development of the image processing algorithms is required for the ability to image uneven terrain. In order to bound the scope of the effort under this contract, the imaging algorithm was designed for level terrain. It may be readily extended to uneven terrain conditions found at some sites as a future task.

During the investigations performed under this contract, it was determined that there is considerable merit in adapting existing imaging techniques to the unique circular spotlight mode operation of the 3-D SISAR. Specifically, there are 3-D imaging techniques being developed at SRI International and the University of Kansas using finite difference time domain methods and computer aided tomography that can be combined with the imaging techniques developed under this contract. In support of the quest to evolve the optimum performing system, it is recommended that the applicability of these methods be explored in future work.

5.3 Platform Migration

The feasibility of stand-off SAR methodology has been demonstrated during this contract. The major system elements of the presently configured 3-D SISAR could be transferred from the towed trailer to other platforms of interest (i.e. truck or airborne) to enhance operational capability.

Migrating the system to a self-contained van or truck is relatively straight forward and would greatly improve the mobility to survey most DOE sites. A complete transfer of the present system with upgrade modification kit could be implemented as a next step in the system evolution.

Since some sites are difficult to access from the ground, it is desirable to adapt the radar for airborne operation. In addition, the airborne system offers great potential for material hazard avoidance. After a careful trade study is completed with the assistance of a helicopter or airplane integrator, a system specification and mechanical designs related to air worthiness would be generated. A simple set of feasibility experiments can be defined to prove the concept and validate the robustness of the system approach.

6.0 References

G. Burke, "Numerical Electromagnetics Code - Method of Moments, User's Guide for NEC-3, LLNL Report

Rogers, J. R., "JRMBOR: Computation of Scattering from a General Body of Revolution," Technical Report JR-2, Vols 1-2 (Atlantic Aerospace Corporation, 26 July 90).

7.0 Acronyms and Abbreviations

List of Symbols, Abbreviations & Acronyms

3-D SISAR	Three-Dimensional Synthetic Aperture Radar
DAS	Data Acquisition Subsystem
FFT	Fast Fourier Transform
FMCW	Frequency Modulated Continuous Wave
GB	Gigabytes
GPR	Ground Penetrating Radar
I & Q	In-phase and Quadrature
KHz	Kilohertz
MB	Megabytes
MHz	Megahertz
MTV	Mirage Test Vehicle
pixel	Picture element, a 2-D picture element
UNIX	A multitasking computer operating system
VME	A hardware packaging and electrical bus
voxel	Volume element, a 3-D picture element

Appendix I. Task Summary

The following is a summary of the Statement of Work tasks. The flow of these tasks is shown in Figure I-1 which is a PERT chart of the major project activities.

a. Systems Engineering

- Performed requirements studies to establish the system and subsystem performance parameters

- Defined the collection geometry, and approaches for the matched filter and target recognition techniques

- Specified the image processing approach and display workstation and software requirements

- Developed models of the target EM scattering behavior and of the underground propagation and clutter phenomena

- Developed a data simulator to model the overall system performance and assist in the evaluation of the motion compensation and imaging algorithm performance.

- Prepared a system test and evaluation plan for the data collection experiments and field tests

b. Hardware Design, Development, and Integration

This task covered the design and development of the demonstration hardware which consists of the antenna system, radar, position location repeaters, and MTV modifications.

- Antenna system design and development, including the selection and procurement of an antenna, rotator, adjustable height mast, and the mast to MTV mounting attachments.

- Design and fabrication of the radar receiver-transmitter, including the circuitry for the generation and reception of all RF and timing signals used by the 3-D SISAR.

- MTV modifications, consisting of the mechanical and electrical integration of the radar and antenna subsystems, the operator's workstation, and power generator into the Mirage Systems MTV.

- Repeater design and construction, consists of the design, fabrication, and test of a set of radar signal repeaters that support the Motion Compensation technique required for the SAR imaging.

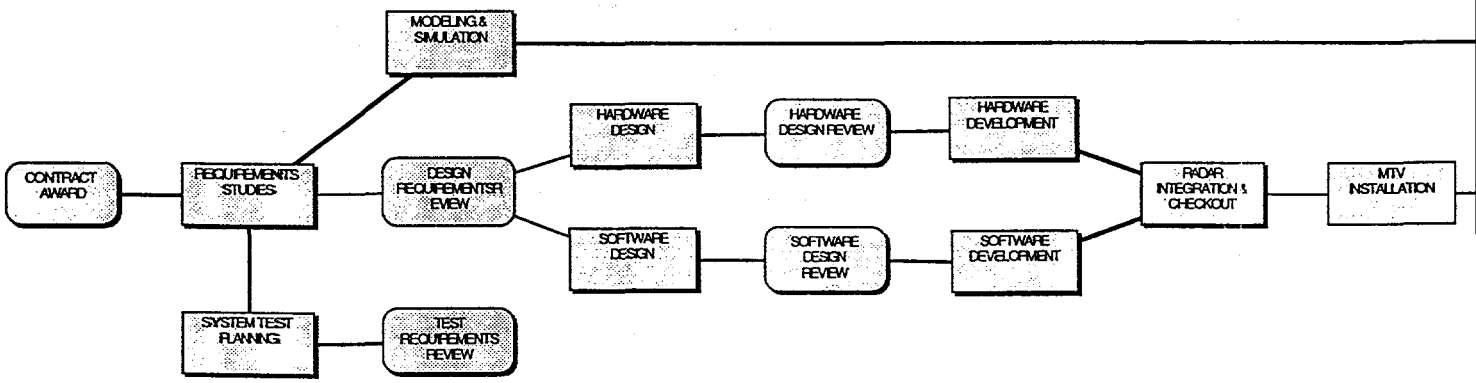
MODELING & SIMULATION
CONTRACT AWARD
REQUIREMENTS STUDIES
DESIGN REQUIREMENTS REVIEW
HARDWARE DESIGN
HARDWARE DESIGN REVIEW
HARDWARE DEVELOPMENT
SOFTWARE DESIGN
SOFTWARE DESIGN REVIEW
SOFTWARE DEVELOPMENT
RADAR INTEGRATION & CHECKOUT
MTV INSTALLATION
SYSTEM TEST PLANNING
TEST REQUIREMENTS REVIEW

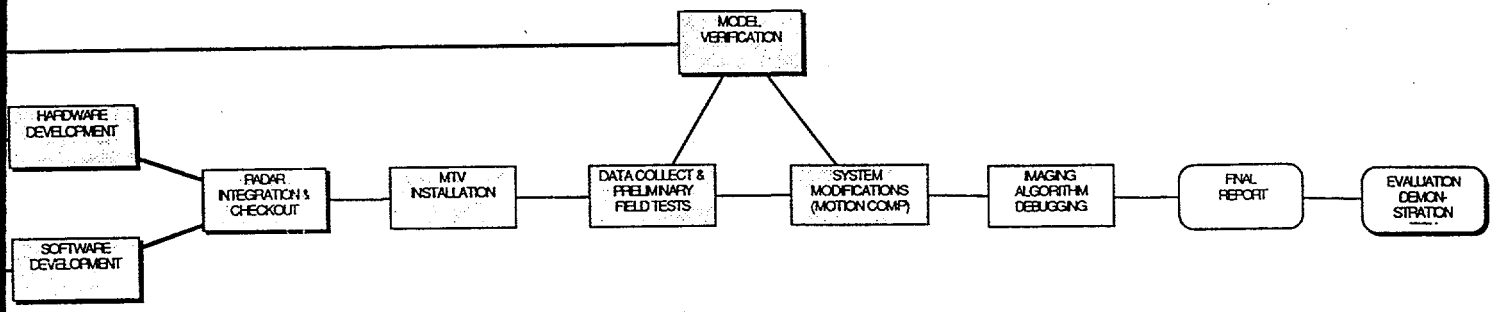

Figure I-1. 3D-SISAR task progression.

c. Data Processing Algorithms and Software Development

The objective of these subtasks is to develop the algorithms and software needed for the processing and control elements of the system.

- Radar Signal Processing and Motion Compensation. The effort under this subtask is to develop the software for radar waveform and data collection processing, including the extraction and processing of the data from the set of repeaters to accurately determine the radar position vs. time for the SAR motion compensation.

- Image Processing. The implementation of the three-dimensional imaging and object recognition and analysis algorithms. The basic image processing will utilize match-filters for object detection, recognition, orientation, and location of desired objects.

- Image Display. The image display function utilizes a three-dimensional imaging software package running on a graphics workstation to provide three-dimensional displays of the imaged data.

- Radar System Control. Develop the software to perform the radar system control, signal collection, and waveform generation.

d. Integration and Checkout - integrate all hardware and software, perform sub-system diagnostic tests and system level performance evaluation to ensure that the total system is functioning properly before and after installation in the MTV. ran system level performance tests locally to ensure that the total system functions properly before the off-site field tests, evaluate imaging algorithm performance and compared with the modeling verification results of the systems engineering subtasks. System performance was optimized after each stage of the evaluation through modifications made to the imaging algorithms and radar operating parameters.

e. System Test and Evaluation

The objective of this task was to perform the necessary experiments and field tests required to fully evaluate the system and to project its performance parameters.

- Data Collection Experiments

The objective of this subtask was to collect radar data primarily to support the system engineering effort. Experiments were conducted for test objects located both above and below ground with generic targets of interest in order to evaluate the performance of the radar under very controlled conditions. These field experiments were run in the San Francisco Bay Area at the Mirage Systems facility in Sunnyvale, CA and at the Stanford

University Geophysics Test Range described in the System Test and Evaluation Plan.

- Preliminary Field Tests

Preliminary field tests serve to validate the system design and to establish the system performance parameters. The testing included the burial of a variety of generic and realistic targets of interest under a variety of conditions ranging from controlled to those likely to be encountered in operation. The data gathered was used to validate and refine the system design, especially that of the motion compensation and imaging algorithms. These field experiments were run at the Mirage Systems prepared site located near Jamestown, CA.

f. Evaluation Field Test

The objective of this subtask is to demonstrate to the DOE the operation and performance of the 3-D SISAR. This test has not yet been conducted, but will be at one of several sites. Candidate sites include the Mirage Systems test facility described in para 2.7.4, the Stanford University geophysics test range, and a DOE test site such as Rabbit Valley, Colorado.

Appendix II. System Description

1.0 System Description

The 3-D SISAR is a Ground Penetrating Radar built for the detection, location, and identification of underground objects and voids. The 3-D SISAR provides enhanced depth penetration ability and an indication of buried object size and shape.

The radar is mounted on a ground-based vehicle, the Mirage MTV. During operation, the radar and antenna are moved along a curved path such as an arc or circle around an area of interest while continuously illuminating the area of interest. A set of three phase reference repeaters are used in a position location system with the radar to enable the coherent processing of the reflections received from buried objects within the area of interest. The radar data is used to build a three-dimensional map describing the location and, where possible, the likely identity and orientation of the buried object.

The radar uses a frequency modulated, continuous wave (FMCW) waveform in a monostatic (single antenna) mode of operation. The transmitter and receiver are alternately connected to the antenna through a Transmit/Receive Switch for short periods of time, generally hundreds of microseconds to several milliseconds. The waveform generator provides the exciter signal for the transmitter and a replica of that signal to the receiver for use as a reference during signal demodulation. The receiver output is digitized and provides two output paths. The first path consists of real-time processing based on the Fast Fourier Transform (FFT) algorithm. The displayed FFT data allows the operator to monitor the data gathering process. The second path consists of a recording capability for the digitized receiver in-phase and quadrature phase (I and Q) outputs for subsequent computer-based 3-D image processing. The signals from the phase reference repeater are embedded within the radar data, and no special hardware is needed to process them.

The image processing is not done while gathering radar data because it entails large amounts of computer based processing to generate the 3-D images. Thus, recorded data gathered by the mobile radar unit is brought to the image processor, a computer workstation described in Para. 3.6.4. The overall process of generating the 3-D images involves the following processing steps:

1. Motion Compensation. The recorded I & Q data from the mobile radar unit includes the returns from the buried object volume including buried objects and clutter, and the reflections from each of the repeaters. The reflections from each repeater yield a direct measurement of the distance of each repeater from the mobile radar unit when the radar receiver data was recorded. The motion compensation process calculates the radar position for each set of buried object data.

2. Matched filtering of the data against a library of scattering functions for the buried objects of interest. By comparing the observed buried object scattering characteristics with the library of known characteristics of various stored buried objects, one can calculate the correlation of the observed scattering with that of known buried object types and orientations. A high degree of correlation is an indicator of the buried object location, orientation, and type.

3. Image display. Using the location and object type data, the display software shall draw a representation of the object at the computed location and orientation on a three-axis map of the underground volume of interest. The map shall contain descriptive information about the object properties.

1.1 Interface Definitions

The system is basically self-contained, from the radar sensor through the signal processing. Control of the operation and data collection functions of the radar are performed by the Data Acquisition Subsystem (DAS). The major internal interfaces are between the DAS and the radar unit, the system calibration equipment, and the computer workstation. The interfaces to the radar unit shall provide control and status functions through an RS-422 data link, and provide a high speed data bus for the transfer of the radar data to the DAS. The interface to the system calibration equipment shall handle communications over an IEEE-488 bus to the frequency counter and power meter. The interface with the computer workstation shall take the form of either an Ethernet data link or a tape cartridge for archiving and storing the collected data. The tape storage provides the medium for transferring the radar data files to the workstation when the workstation is located at a facility away from the data collection site.

2.0 Characteristics

2.1 Performance Characteristics

The 3-D SISAR provides the following performance:

Detection depth	up to 10 meters
Types of objects detectable, minimum set	Drums, pipes, plates, test spheres
Position location error, in x, y, and z:	One foot near surface, increasing with depth according to local soil conditions.
Frequency Range:	20-1,000 MHz

Waveform Type:	Interrupted FMCW, 50% duty cycle

2.2 Physical Characteristics

The radar unit and antenna is installed on a telescoping mast attached to the roof of the MTV. The equipment necessary to operate the radar, including the Data Acquisition Subsystem, power supplies, performance monitoring equipment, and AC power generator, are installed within the MTV. Principle characteristics of the system components are:

Radar unit

Enclosure type:	Weatherproof, sealed, EMI shielded drawn aluminum enclosure with integral air-air heat exchanger, reflective white painted finish
Dimensions:	18" X 18" X 8"
Weight:	35 pounds

Antenna

Type:	Split-boom log-periodic design
Length:	16 foot boom length
Weight:	75 pounds, max

Telescoping mast

Type:	Heavy-duty, pneumatically operated mast with locking collars to enable the mast to be set to intermediate heights
Extended length:	30 feet, fully extended

Antenna rotator

Type:	Elevation over azimuth configuration, with remote control and indicator
Weight:	15 pounds
Axis travel:	360° azimuth ±60° elevation

Radar unit power supply

Description:	Rack-mountable chassis
Dimensions:	19 " W X 21" D X 8-1/2" H
Weight:	35 pounds

Data Acquisition Subsystem

Computer chassis:	Rack-mountable VME chassis
Dimensions:	19" W X 24" D X 8-1/2" H
Weight:	50 pounds
Monitor:	High resolution RGB display
Screen size:	19"
Weight:	75 pounds

2.3 Environmental Conditions

The components of the 3-D SISAR system that are mounted on the exterior of the MTV (mast, antenna, rotator, and radar unit) are operable over the following range of environmental conditions:

Temperature:	0-45 °C
Relative humidity	0-90 %

The system is resistant to the effects of rain, dust and dirt, non-salt fog, and direct sunshine.

Components of the 3-D SISAR system that are installed within the interior of the MTV (Data Aquisition Subsystem, power supplies, calibration equipment, air compressor, AC generator, etc.) are operable over the following range of environmental conditions:

Temperature:	10-33 °C
Relative humidity:	0-80 %, non-condensing

2.4 Transportability

The 3-D SISAR system has been installed in a trailer (the MTV) that is transportable by towing over public roads to the test facilities where the system testing takes place. At the test facilities, the MTV is towable over prepared surfaces, i.e., smooth, firm ground.

3.0 Design and Construction

Standard commercial practice construction techniques have been used. Weather resistant materials, coatings, and assembly methods are employed for components of the 3-D SISAR system that are mounted on the exterior of the MTV, i.e., the pneumatic mast, antenna, antenna rotator, and the radar unit.

4.0 Computer Programs

Computer software has been developed in both the C or FORTRAN languages, as appropriate for the application.

5.0 Functional Characteristics

5.1 Radar Characteristics

The radar control is capable of a variety of system operational modes selectable via the Data Acquisition Subsystem user interface. It operates as a phase coherent system, which is necessary to preserve the phase and amplitude signatures produced by the scattering of the radar signals from buried objects.

5.1.1 Transmitter

The transmitter generates the radar signal and amplifies it to the level suitable for transmission. It incorporates provisions for blanking over several frequency segments of each sweep so that nearby communication or navigation systems will not experience interference form the 3-D SISAR. In addition, the transmitter incorporates a power programming feature to linearly reduce the power output below 400 MHz for burnout protection of the T/R switch. Provisions are included for signal sampling by a power meter and frequency counter to support system calibration and self-test.

Output signal	Swept interrupted CW signal, sawtooth sweep pattern, frequency increasing with time.
Instantaneous bandpass	20-1000 MHz.
Power Output:	4 Watts (+36 dBm), peak 2 Watts (+33 dBm), average

5.1.2 Receiver

The 3-D SISAR receiver is a high dynamic range superhet utilizing frequency upconversion for image suppression. It incorporates a transmitter-off mode for performing a scan of the environment to determine frequency occupancy and the presence of any strong environmental signals that could potentially interfere with the 3-D SISAR operation.

Instantaneous, Spurious-free Dynamic Range:	90 dB
Noise Figure:	12 dB

IF frequency	2 GHz
Input attenuator:	Programmable over range of 40 dB in 6 dB steps

5.1.3 Transmit-Receive Switch

The function of the T/R switch is to alternately connect the transmitter and receiver to the antenna, producing the interrupted CW mode of operation. The isolation, losses, and speed of response of this switch are critical to the operation of the radar, and are as follows.

Description:	SPDT equivalent contact arrangement
Isolation:	50 dB from Tx to Rx port during transmit 60 dB from Tx to Rx port during receive
Insertion loss:	1.5 dB, max between antenna port and either Tx or Rx port when selected
Switching speed:	75 nsec, max (recovery time to 2 dB loss or less)

5.2 Antenna and Mast Characteristics

The antenna serves as the radiating element for the system, launching the electromagnetic waves that propagate through the air, into the ground and back. The chief characteristics of this system element are as follows.

Antenna Type:	Split boom, vertically polarized LPA
Frequency coverage:	20-1000 MHz
Gain:	-5 dBi @ 20 MHz to +8 dBi @ 100 MHz and above
Main beamwidth, 3 dB:	60°, in both E- and H-planes

The antenna system and radar unit are mounted on a pneumatic mast which permits adjustment of the antenna height in approximately six foot increments up to a maximum of 30 feet above the roof of the MTV. The antenna is attached to the mast with dual axis (elevation over azimuth) rotator. The rotator position is adjustable via a controller inside the MTV, and the controller has an angle readout of antenna position.

5.3 Repeater Characteristics

Two designs of repeaters were constructed, one active and one passive.

5.3.1 Passive Repeaters. The three passive precision reference repeaters have the following characteristics.

Type	Passive monopole reflector, with pseudo-Doppler modulation
Frequency range	500-1000 MHz
Radar cross section	-20 dBsm on Doppler peaks
Pseudo-Doppler modulation	Square-wave modulation with crystal stability.
Group delay	<1 nsec
Size and weight	8 inch height, 18 inch diameter base, 3 lbs weight with batteries

5.3.2 Active Repeaters. The three active precision reference repeaters have the following characteristics.

Type	Monopole antenna, with pseudo-Doppler modulation added to regenerated sample of incident signal.
Frequency range	500-1000 MHz
Radar cross section	Approx 0 dBsm on Doppler peaks
Pseudo-Doppler modulation	Square-wave modulation with crystal stability.
Signal delay	Approx. 50 nsec
Size and weight	8 inch height, 18 inch diameter base, 3 lbs weight with batteries

5.4 Data Acquisition Subsystem

The Data Acquisition Subsystem (DAS) provides the control, real-time performance monitoring, and data collection functions for the radar. The DAS employs a VME bus based processor utilizing the UNIX operating system, and

incorporates the interfaces needed to exercise its functions and sufficient storage capacity for several data collection runs.

All radar system operating parameters are easily accessible via software control. The operator interface is a windowed display with easy to enter and read system parameters. Graphical displays of the collected radar data are included to assist the system calibration, the setting of radar parameters, and the validation of the correct functioning of the system. Key subsystem parameters are:

Processor:	Sun Microsystems SPARC 5 equivalent
Display size:	19 inch color monitor to accommodate the display of multiple windows simultaneously.
Interfaces:	IEEE-488 bus for control of radar calibration test equipment. RS-422 for radar unit control High speed data bus for radar data

5.5 Three-Dimensonal Digital Imaging Workstation

A computer workstation performs the calculation of the three-dimensional, color-coded maps of the underground region of interest. The workstation permits variable perspective viewing of the mapped underground region. A Tektronix model 4694SX color printer provides paper copies and transparencies of the workstation displays. The workstation is a model Indigo XZ manufactured by Silicon Graphics having the following features:

CPU clock speed:	150 MHz
RAM memory:	96 Mbytes
Hard drive capacity:	1, 2 and 4 Gbyte hard drives
Auxiliary media:	CD ROM reader

5.6 Test Vehicle Characteristics

The 3-D SISAR is housed in and transported by the Mirage Test Vehicle (MTV). The MTV is a custom built trailer capable of supporting a pneumatically assisted telescoping mast for the antenna system and radar unit. An AC power generator was built into the MTV for the source of prime power for the system during field operation. The generator has sufficient capacity to supply the 3-D SISAR power requirements as well as the other MTV loads, including the air

compressor for the pneumatic mast, the air conditioning & heating, lighting, and test equipment.

MTV storage capability:	Able to store the partially disassembled antenna system internally for transport
AC Generator:	5 kW continuous load capacity, gasoline fuel

A suitable table for extended operation is provided for the operator's position.

5.7 Prime Power Characteristics

The 3-D SISAR operates from either commercial AC power or from the generator built into the MTV. The system is operable with power having the following characteristics.

Voltage:	120 VAC, ±10%, 60 ±3 Hz
Maximum system load:	2 KVA @ 60 Hz
Line conditioning:	EMI filter with separate isolation transformer for common mode rejection